THE AMERICAN MINERALOGIST

JOURNAL OF THE MINERALOGICAL SOCIETY OF AMERICA

Vol. 30 SEPTEMBER-OCTOBER, 1945 Nos. 9 and 10

SOAP CRYSTALS

M. J. BUERGER,

Massachusetts Institute of Technology, Cambridge, Massachusetts.

CONTENTS

ABSTRACT

Although soap is crystalline, little is known of the characteristics of soap crystals This paper records an *x*-ray and optical investigation of certain soaps which have been prepared in single crystal condition. These include the α form of the neutral sodium soaps, and the α and β forms of the 1:1 acid sodium soaps. The *x*-ray investigation was carried out by the new precession method of photographing the reciprocal lattice, which is especially adapted to the investigation of crystals with very large cell dimensions. The large cell dimension of soap crystals ranges in the neighborhood of 50 to 100 Å. All data are collected in Table 1.

The several kinds of soap crystals examined to date display great similarities in optical properties, in elastic and plastic properties, and in twinning, in spite of great differences in cell dimensions cell shape, and cell symmetry. This is a consequence of the layer nature of the structures of the crystals.

Introduction

It has recently been established that commercial soaps are aggregates of crystals. This knowledge has brought with it the realization that the properties of various kinds of soaps depend not only on the chemical composition but also on the kinds of crystalline phases present, together with their fabric. Soap manufacture may accordingly be guided by a science of phase fields and phase textures somewhat similar to the science of metallography.

The properties of the various phases of soap are comparatively unknown. One reason for this is that the crystalline nature of soaps has been recognized for a rather short time, but there are also properties inherent in soap which by their very nature hinder the investigation of its crystals. The first is that soap crystals, as a rule, are extremely difficult to prepare in large enough and perfect enough individuals to permit critical examination. The second is that the ordinary methods of x-ray investigation, suitable to the simple inorganic crystals of modest cell dimensions, fail when applied to crystals having the comparatively large cell dimensions of soap crystals.

The present paper reports some crystallographic and optical properties of certain soap crystals which it has been possible to prepare in single crystals suitable for investigation. The crystals used by the writer for the investigation herein reported were prepared at the Research Laboratory of Lever Brothers, Cambridge, under the direction of Dr. L. B. Smith. The writer is especially indebted to Messrs. F. V. Ryer and K. W. Gardiner for their patient efforts to provide suitable material.

Methods of Investigation

X-ray investigation. The symmetry and cell dimensions were obtained by means of a novel x-ray diffraction method, the *precession method.*[1] This technique is ideally suited to the study of very large unit cells such as occur among soap crystals. This is because *precession photographs* are simply scaled replicas of levels of the reciprocal lattice. To interpret them, one needs but inspect them for symmetry, lattice type, systematic absences of points (for space group determination), and, finally, make comparatively simple measurements of certain dimensions of the re-

[1] Buerger, M. J., The photography of the reciprocal lattice: *ASXRED Monograph* **1** (August, 1944).

ciprocal lattice for transformation into direct cell dimensions.

Soap crystals have such large cells that the reciprocal cells are composed of rows of very closely spaced points. If a reciprocal cell of this kind is recorded by the usually powerful Weissenberg method, the interpretation of the photographs is tedious, and there is very real danger of misinterpretation because the errors in transforming a Weissenberg projection into a map of the reciprocal lattice are of about the same order of magnitude as the spacing of points in the reciprocal lattice rows themselves. Transformation errors are entirely avoided in the precession method because no transformation is necessary; the photographs themselves are scaled replicas of the various levels of the reciprocal lattice.

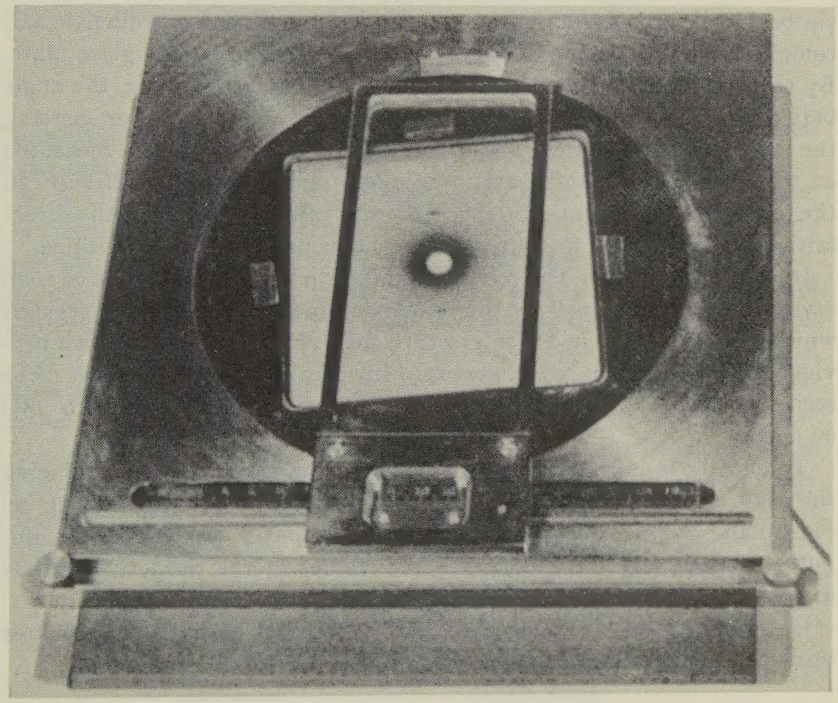

FIG. 1

Inter-row angles and inter-row spacings on precession photographs are measured with the aid of a device which is similar to an instrument described previously[2] for measuring distances and spacings on films. The new device can also measure angles. In both the earlier instrument and

[2] Buerger, M. J., *X*-ray Crystallography (John Wiley, New York, **1942**) Fig. 229, p. 446.

the new one, spacings are measured as follows: The photograph to be measured is placed under a movable glass plate in such a way that a row of spots in the photograph is aligned along a hair line engraved on the under surface of the glass plate. The coordinate of the line is then measured by means of a millimeter scale and vernier. The plate is then moved parallel with itself until the engraved line comes to coincide with another parallel row of spots on the film, and the coordinate of the line is again read. The difference in the two coordinates is the spacing of the parallel rows on the photograph.

In the new device, Fig. 1, this principle is the same, but the photograph may also be rotated beneath the glass plate by means of a rotating stage similar to a rotating microscope stage. By means of this motion, reciprocal lattice rows of any direction can be brought into parallelism and coincidence with the line of fixed direction engraved on the glass plate. By reading the initial and final angular positions of the stage, the angle between two reciprocal lattice rows can be determined. Thus, in general, the interaxial angles α^*, β^*, and γ^* can be selected and directly measured on the a axis, b axis, and c axis precession photographs respectively. In the monoclinic case, since $\beta = 180° - \beta^*$, the interaxial angle of the direct lattice can be directly measured on the b axis precession photographs.

Optical investigation. The refractive indices α and β for the several soap crystals were determined by the immersion method, using soap crystals which appeared large in the microscope field of view. Liquids which provided final matches in index were immediately standardized on an Abbe refractometer. The α and β indices are believed to be accurate to .003 or better.

To find the index γ directly by the immersion method requires placing the soap flake on edge. This is difficult to accomplish with crystals as plastic and as fragile as soap crystals. The index γ was therefore computed in each case from the measured values in the refractive indices α, β, and the optic angle, V, in the usual way.

Optic angles were measured by the method of Mallard. The values probably contain errors of the order of 5°.

The α Neutral Sodium Soaps

Symmetry and cell. The geometrical features of the "alpha" form of the neutral sodium soaps have already been discussed.[3] This form was first regarded as anhydrous,[4] but has subsequently been shown to be a

[3] Buerger, M. J., The characteristics of soap hemihydrate crystals: *Proc. Nat. Acad. Sci.*, **28**, 529–535 (1942).

[4] Thiessen, Peter A., and Stauff, Joachim, Feinbau und Umwandlungen kristallisierter Alkalisalze langkettiger Fettsäuren: *Zeit. Physikal. Chem.*, (*A*) **176**, 397–429 (1936).

hemihydrate.[5] There is now abundant unpublished evidence confirming the hydrated character of the so-called "alpha" form of the neutral sodium soaps. Sodium palmitate, stearate, behenate, and arachidate have been produced[7] in the "alpha" form.

"Alpha" sodium stearate hemihydrate has been restudied by the powerful precession method. Precession photographs of the reciprocal lattice are shown in Fig. 2. The following plane symmetries are evident:

Precessing axis	Level	Symmetry
c	zero	*ll*
b	zero	2
	n	2
a	zero	*ll*
	n	*l*

These data fix the point group as $2/m$ and consequently place the crystal in the monoclinic system.

By laying a horizontal straight edge on the *a* axis *n* level photographs, it is evident that the (100)* nets are diamond, which calls for an *A*-centered lattice. The zero level (010)* net has alternate [100]* rows missing, which requires a glide *a*. There are no other systematic omissions of reciprocal lattice elements. This information fixes the diffraction symbol as $2/mA-/a$. This diffraction symbol permits either of the space groups Aa or $A2/a$ as possibilities. If the crystal is indeed a hemihydrate, the number of water molecules per unit cell is exactly enough to fill the general positions of the more symmetrical space group, but too many to fill the general positions of the less symmetrical space group. The most likely space group is therefore $A2/a$.

The cell dimensions for "alpha" sodium stearate hemihydrate are:

a	9.16 *kX*
b	8.00
c	103.96
β	$93\frac{1}{4}°$
cell content	$16NaSt.\frac{1}{2}H_2O$
computed density	1.10

The morphological and plastic properties of these crystals have already been reported.[3]

Optical properties. The optical properties of the "alpha" form of the stearate[6] and palmitate[6] are as follows:

[5] Buerger, M. J., Smith, L. B., de Bretteville Jr., A., and Ryer, F. V., The lower hydrates of soap: *Proc. Nat. Acad. Sci.*, **28**, 526–529 (1942).

	α NaSt·$\frac{1}{2}H_2O$	α NaP·$\frac{1}{2}H_2O$
refractive indices α	1.507	1.505
β	1.517	1.517
γ	1.56*	1.57*
optic angle		
$2V$ (in crystal)	49°	50°
$2E$ (in air)	78°	80°
dispersion	$r>v$ marked	$r>v$ strong
optical orientation	$X=b$	$X=b$
	$Y\approx a$	$Y\approx a$
	$Z\approx c$	$Z\approx c$

* Computed from α, β, and V.

The α 1:1 Acid Sodium Soaps

Introduction. The 1:1 acid soaps such as HSt·NaSt, occur in two forms, here designated α and β. Such soaps can be prepared,[7] for example, by cooling solutions made by dissolving equimolar portions of fatty acid and soap in 95% alcohol. If the precipitation takes place above a critical temperature, the β form appears; if below the critical temperature, the α form appears. The critical temperature for HSt·NaSt is about 50°C.

The α form has been prepared[7] for HMy·NaMy, HP·NaP, HSt·NaSt, HBh·NaBh, HAr·NaAr, and for the mixed acid soaps HP·NaSt and HSt·NaP.

Habits. The habit of HSt·NaSt crystals precipitated from 95% alcohol solutions is somewhat elongated tabular, with the ratio of length ($\|a$) to width ($\|b$) about 2:1. When precipitated from a solution containing excess fatty acid, this ratio increases so that the crystals become acicular, and tend to occur in sheaves. Crystals precipitated from solutions containing an excess of dissolved soap, on the other hand, tend to have a length to width ratio perhaps slightly smaller than for those precipitated from exactly equimolar solutions.

---

[6] The following abbreviations are used in this paper for organic radicals:

Composition	Name	Abbreviation
$C_{12}H_{24}O_2$	laurate	L
$C_{14}H_{28}O_2$	myristate	My
$C_{16}H_{32}O_2$	palmitate	Pa
$C_{18}H_{36}O_2$	stearate	St
$C_{20}H_{40}O_2$	arachidate	Ar
$C_{22}H_{44}O_2$	behenate	Bh

[7] The preparations of all crystals discussed in this paper were carried out by Messrs. F. V. Ryer and K. W. Gardiner, to whom the writer is indebted for this information.

Since an elongated tabular habit is also one of those exhibited by "alpha" NaSt·$\frac{1}{2}H_2O$, it will be useful to point out that these two crystals, though somewhat similar in habit, can be distinguished on the basis of optical elongation. NaSt·$\frac{1}{2}H_2O$ is customarily elongated parallel to the optical direction X, and consequently has negative elongation as seen looking normal to the tablet. On the other hand, the α HSt·NaSt and α HP·NaP crystals are elongated parallel to the optical direction Y and consequently exhibit positive elongation when viewed normal to the tablet. (Not only are the neutral hemihydrates monoclinic, but the symmetry studies, noted beyond, prove that the alpha acid soaps are also monoclinic. The neutral soaps are customarily elongated parallel to the two-fold axis, while the acid soaps are customarily elongated at right angles to the two-fold axis.)

Symmetry and cells. For the precession method, these crystals are most easily investigated by mounting them so that the axis of greatest elongation is parallel with the glass capillary to which the crystal is attached. When the crystal is mounted in the usual adjusting crystal holder and placed on the precession instrument, it can accordingly be rotated about the zone of elongation. Thus, the flat surface of the crystal can be brought either normal or parallel to the precessing axis.

As a matter of general strategy in the precession investigation of any soap crystal, the normal to the flat surface (which has never proven to be a rational direction, although in cases studied so far, it has always turned out to be within a few degrees of c) is first brought parallel with the precessing axis. In the case of the α acid soap crystals, this gives a photograph shown in Fig. 3*A* (photographs of acid palmitate and acid stearate cannot be distinguished). This photograph records the projection in this nearly rational direction, not only of the zero level, but also of the first level, since in the particular instrumental adjustment employed, a wide layer-line opening was used. From this photograph, symmetry information and dimensional information can be obtained which is especially valuable for making n-level settings for subsequent photographs. When the flat surface of the crystal is adjusted parallel with the precessing axis, a cone axis photograph[1] proves to be centered, showing that this new direction is rational. The zero and first levels of the reciprocal lattice normal to this axis and as photographed by the precession method are shown in Figs. 3*B* and 3*C*.

FIG. 2. Precession photographs of α NaSt. Figs. 2*A*, 2*B*, and 2*C* represent three central sections of the reciprocal lattice, in correct relation: Figs. 2*A* and 2*B* have a central horizontal line in common, and Figs. 2*A* and 2*C* have a central vertical line in common. Fig. 2*D* is a section parallel to that of Fig. 2*C*, but at another level. Note the symmetries of the levels, and compare Fig. 2*C* with Fig. 2*D* for extinguished rows.

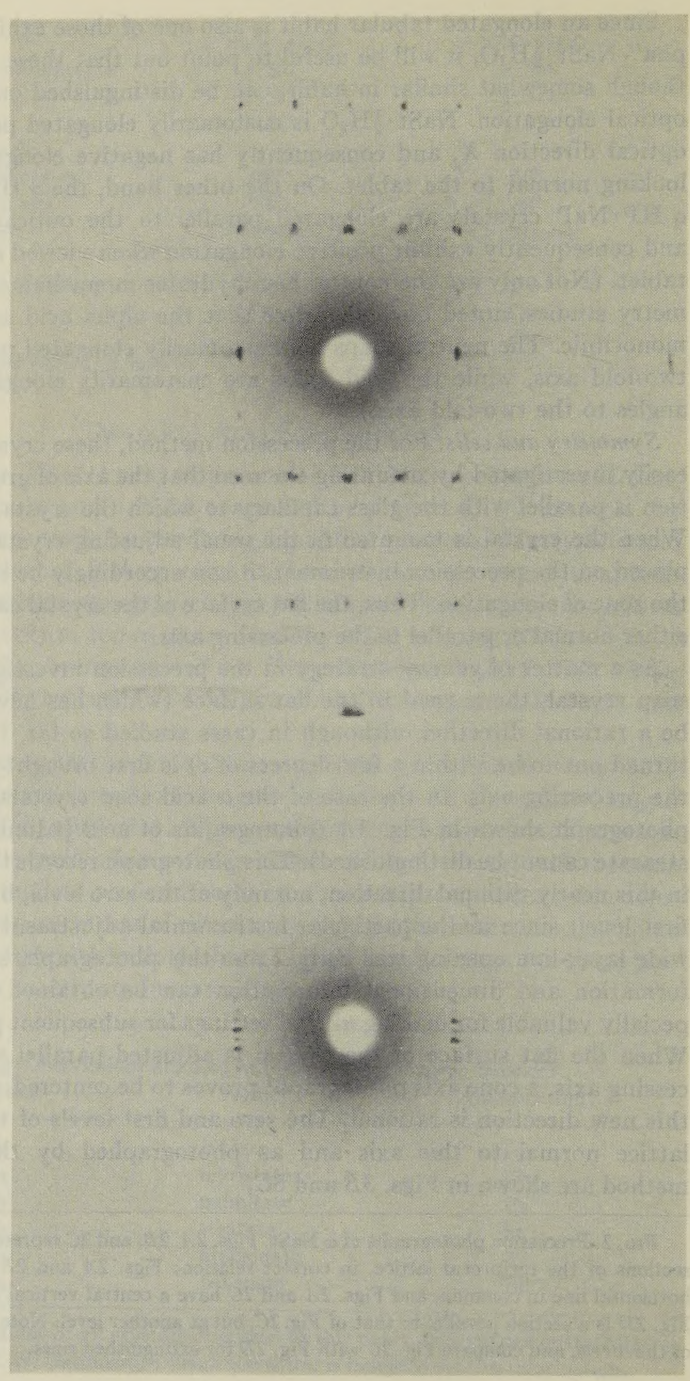

Fig. 2A.
c axis,
several levels.

Fig. 2B.
b axis,
zero level.

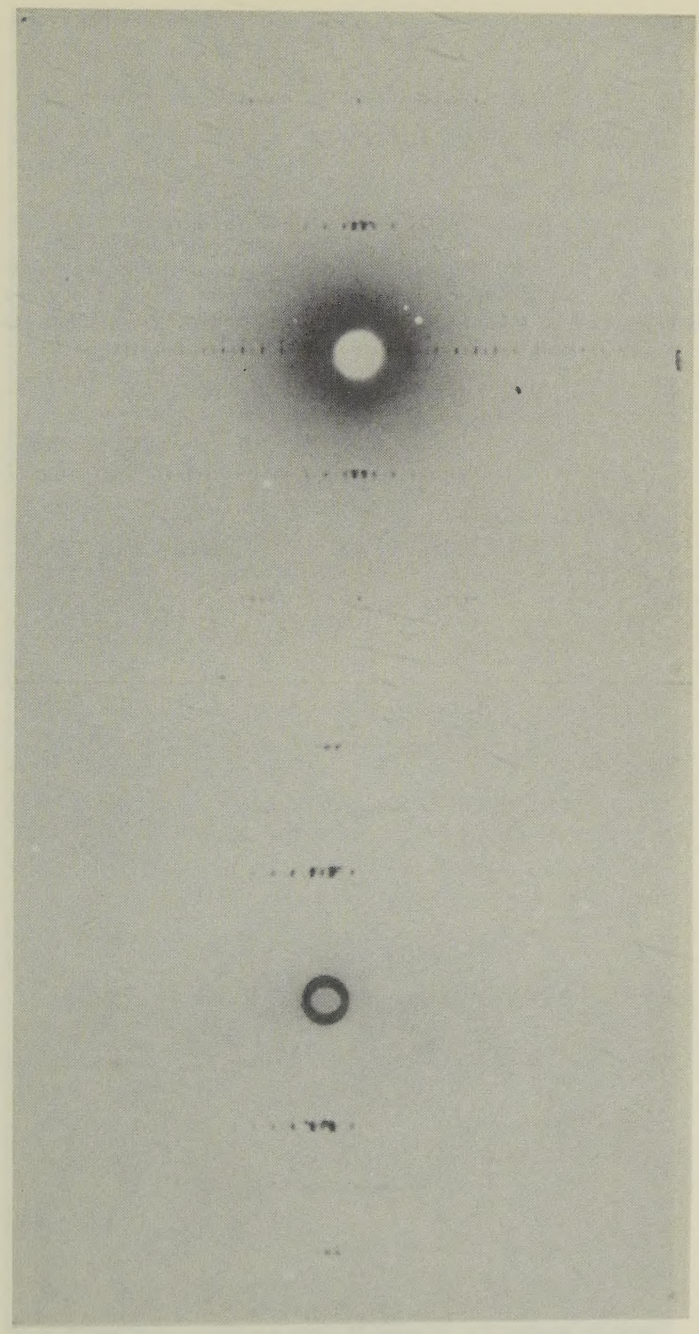

Fig. 2C.
a axis,
zero level.

Fig. 2D.
a axis,
1st level.

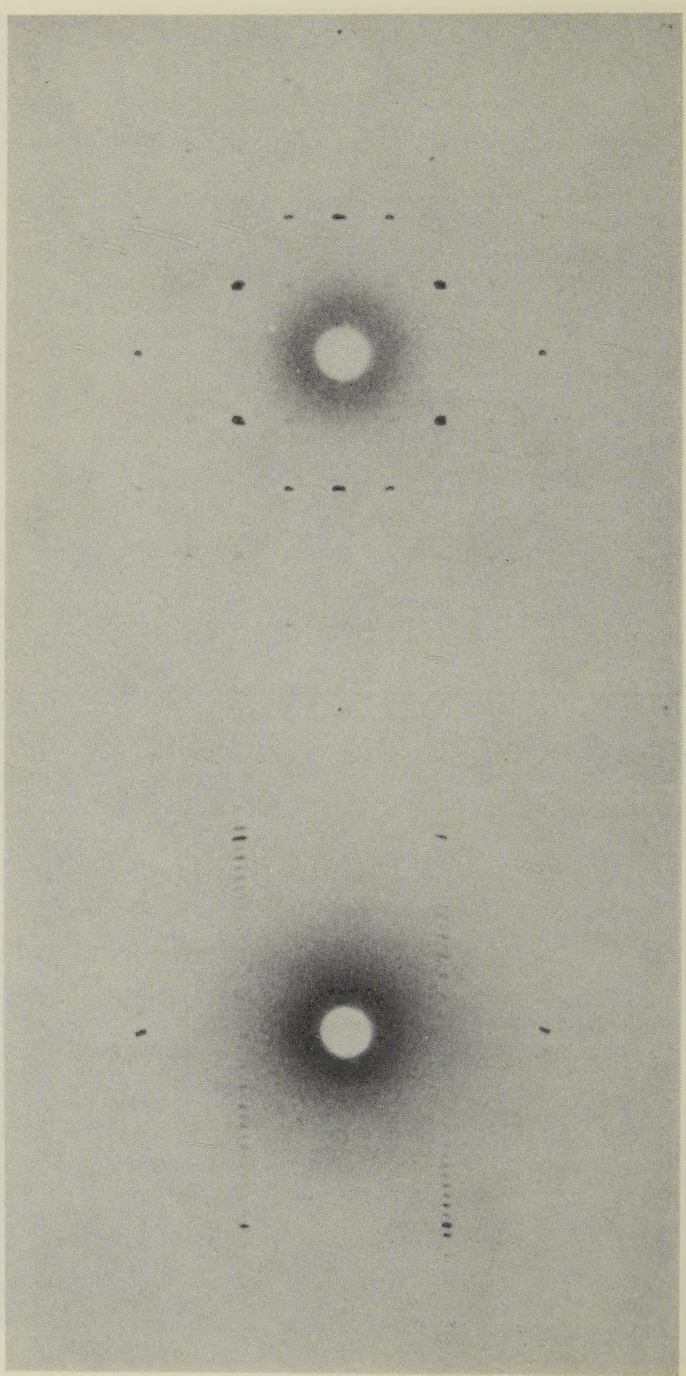

Fig. 3A.
c axis,
several levels.

Fig. 3B.
b axis,
zero level.

FIG. 3. Precession photographs of α HSt · NaSt. Figs. 3*A* and 3*B* represent central sections of the reciprocal lattice, in correct relation; they have a central horizontal line in common. Fig. 3*C* is a section parallel to that of Fig. 3*B*, but at another level. Note the symmetries of the levels, and compare Fig. 3*B* with Fig. 3*C* for extinguished lattice rows.

Fig. 3C.
b axis,
1st level.

The symmetries displayed by these three photographs are evidently as follows:

Fig.	precessing axis	level	symmetry	axial label
3A	⊥ plate	0+1	*ll*	$\approx c$
3B	∥ plate	0	2	*b*
3C	∥ plate	1	2	

These symmetry data are sufficient to prove the diffraction point group to be $2/m$. (This symmetry was confirmed by transferring the crystal, as mounted, to a de Jong-Bouman apparatus and rotating about the long, or *a*, axis of the plate. The zero level symmetry was *ll* while the first level symmetry was *l*.)

By superposing the zero level and *n*-level, *b* axis precession photographs (Figs. 3*B* and 3*C*) it is evident that the cell is not centered, hence primitive. Comparing the two photographs shows that the a^* translations are doubled on the zero level, indicating a glide, *a*. Also, the b^* translation on the central line of the *c* axis photograph (Fig. 3*A*) is doubled, indicating a screw 2_1. The diffraction symbol is accordingly $2/mP2_1/a$. This embraces only one space group, namely $P2_1/a$.

The cell dimensions of the α acid sodium palmitate and α acid sodium stearate, as determined from precession photographs, are as follows:

	α HP·NaP	α HSt·NaSt
a	9.97 *kX*	9.97*kX*
b	7.38	7.38
c	45.7	50.7
β	93°	92¾°
cell contents	4 (HP·NaP)	4(HSt·NaSt)
computed density	1.05	1.05

Mechanical properties. Like $NaP \cdot \frac{1}{2}H_2O$ and $NaSt \cdot \frac{1}{2}H_2O$, the acid sodium soap crystals have perfect (001) cleavage as well as perfect (010) cleavage. Similarly, the acid soaps also display very easy plasticity with translation-gliding plane $T=(001)$. It is difficult, however, to discover a folding axis for the plate; hence it may be assumed that any direction in (001) may function as the gliding direction, *t*.

Optical properties. The optical properties of the α form of the sodium acid soaps are as follows:

		α HP·NaP	α HSt·NaSt
refractive indices	α	1.501	1.506
	β	1.513	1.516
	γ	1.57*	1.56*

optic angle	α HP·NaP	α HSt·NaSt
$2V$ (in crystal)	49°	49°
$2E$ (in air)	78°	78°
dispersion	$r>v$ marked	$r>v$ marked
optical orientation	$X=b$	$X=b$
	$Y\approx a$	$Y\approx a$
	$Z\approx c$	$Z\approx c$

* Computed from α, β, and V.

The β 1:1 Acid Sodium Soaps

Introduction. The higher temperature form of the 1:1 acid soaps is here designated β. This form has been prepared[7] for HP·NaP, HSt·NaSt, HBh·NaBh, HAr·NaAr, and for the mixed acid soaps, HP·NaSt and HSt·NaP. Data are given here for β HSt·NaSt only. This may be prepared, for example, by precipitation from a 95% alcohol solution above about 50°C. The present study was made on cleavage flakes of irregular outline.

Symmetry and cell. A precession photograph was first made with the precessing axis normal to the plate. The photograph is shown in Fig. 4*A*. Evidently the symmetry is 2, which is lower than in the cases of the two soaps previously described. The plane of the cleavage is, of course, rational and therefore contains two possible unit translation vectors. In conformity with usage adopted for other soap crystals, these translations are designated a and b, with c becoming transverse to the plate. Provided that c is approximately normal to the plane of the plate (as, indeed, it subsequently develops), then a^* and b^* are also approximately in the plane of the plate, and Fig. 4*A* then presents a photograph of a projection of (001)* which differs little from a parallel projection. Hence, a^* and b^* can be selected from Fig. 4*A*, and, with the proviso above mentioned, rather good values of a, b, and γ can be measured.

With a^* and b^* selected from Fig. 4*A*, the angle which each of these makes with the horizontal universal joint shaft of the precession instrument can be measured. The measurement required is merely the angle between the reciprocal lattice row and the horizontal edge of the film, and this measurement is easily made with the device shown in Fig. 1. When these angles are known, the crystal can be adjusted by means of an arc of the adjusting crystal holder (with the crystal remounted if the adjustment is beyond the range of adjustment of the arc) so that a^* (say) is parallel with the horizontal edge of the film. If, now, the crystal is rotated 90° about the horizontal axis, a^* remains horizontal, c^* comes approximately into the plane of the film, and b becomes nearly parallel

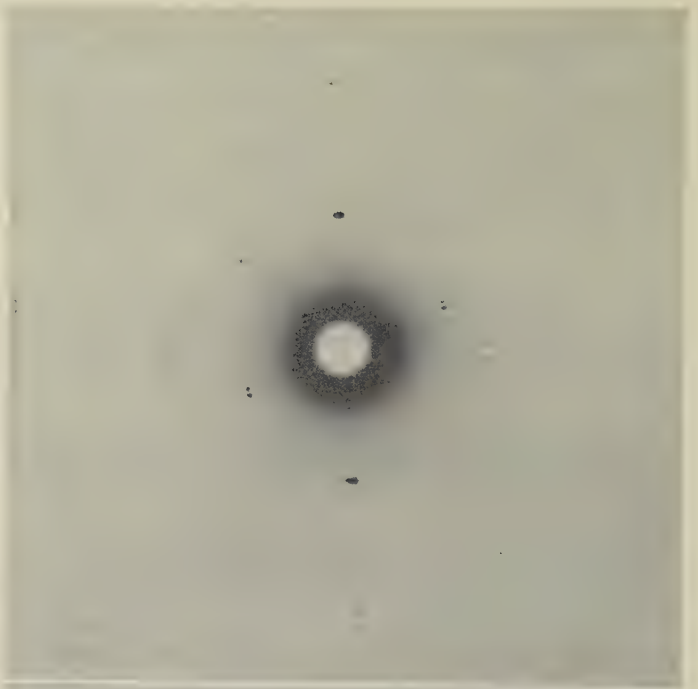

Fig. 4A.
c axis,
several levels.

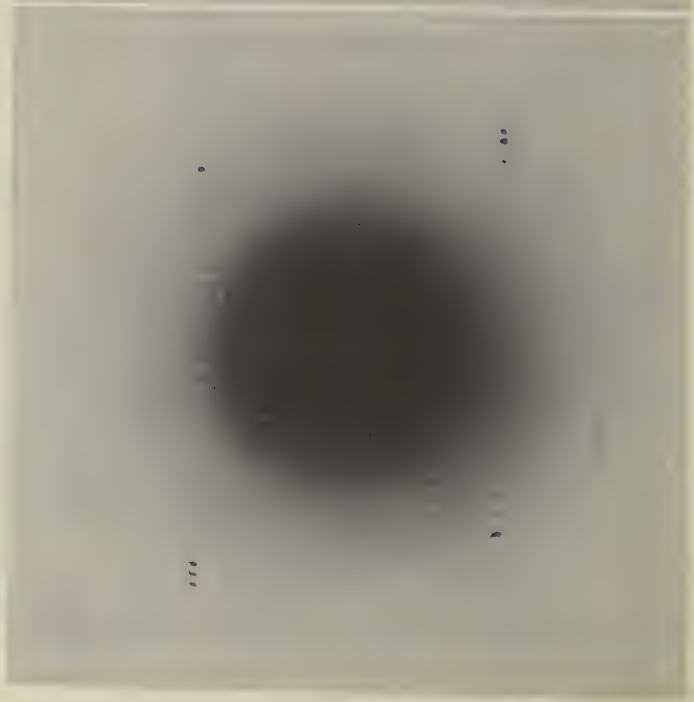

Fig. 4B.
b axis,
zero level.

FIG. 4. Precession photographs of β HSt · NaSt. Figs. 4*A* and 4*B* represent central sections of the reciprocal lattice, in correct relation; they have a central horizontal line in common. Fig. 4*C* is a section parallel to that of Fig. 4*B*, but at another level. Note the symmetries of the levels. Note also the central blind spot in Fig. 4*C*, which is a characteristic of upper-level photographs. Fig. 4*B* was deliberately overexposed in order to record a weak level.

Fig. 4C.
b axis,
1st level.

to the precessing axis. Photographs made with b thus adjusted very approximately parallel to the precessing axis are shown in Figs. 4*B* and *C*.

The symmetries involved in the several photographs of Fig. 4 are evidently 2 for the zero level and 1 for each n-level. The crystal is thus triclinic, with space group either $P1$ or $P\bar{1}$.

Because the crystal used had only one developed surface, namely the (001) cleavage of the flake, and because the distribution of reflections was inappropriate to the precession method of orienting the crystal,[1] small orientation errors, of the order of a few degrees, existed between the reciprocal lattice and its photographs, Fig. 4. Consequently it was impossible to obtain very exact values of the cell dimensions, especially with regard to angles, and the latter may be in error by a degree or so. The cell dimensions so obtained were:

$a = 9.98\ kX$	$\alpha = 90\frac{3}{4}°$
$b = 11.46$	$\beta = 90°$
$c = 50.2$	$\gamma = 94°$
cell contents 6(HSt · NaSt)	
computed density 1.02	

Mechanical properties. β HSt · NaSt has perfect (001) cleavage, as other soaps, and also perfect (110) cleavage. It is somewhat less plastic than the two previously described crystals, with $T = (001)$, t unknown.

Optical properties. The optical properties of the β form of sodium acid stearate are as follows:

		HSt · NaSt
refractive indices	α	1.498
	β	1.510
	γ	1.59*
optic angle		
$2V$ (in crystal)		42°
$2E$ (in air)		66°
dispersion		$r > v$ marked
optical orientation		$X \wedge b = +40°$
		$Y \wedge a = +36°$
		$Z \wedge c = 90°$
		$X \wedge (110)$ (cleavage) $= -11°$

* Computed from α, β, and V.

Remarks on Some Properties of Soap Crystals

Tabulated data. For convenience, the cell, mechanical, and optical properties of the several soap crystals are brought together in Table 1.

Powder photographs of soap crystals. Powder patterns of soap crystals are easily made with the aid of what amounts to a hollow needle.

TABLE 1

			α Neutral Sodium Soap Hemihydrate		α 1:1 Acid Sodium Soaps		β 1:1 Acid Sodium Soap
			$NaP \cdot \frac{1}{2}H_2O$	$NaSt \cdot \frac{1}{2}H_2O$	$HP \cdot NaP$	$HSt \cdot NaSt$	$HSt \cdot NaSt$
Crystallographic properties	Crystal System Space group		Monoclinic Aa or $A2/a$		Monoclinic $P2_1/a$		Triclinic $C1$ or $C\bar{1}$
	Cell dimensions	a	9.13 kX	9.16 kX	9.97 kX	9.97 kX	9.98 kX
		b	8.01	8.00	7.38	7.38	11.46
		c	91.85	103.96	45.7	50.7	50.2
		α					$90\frac{3}{4}°$
		β	94°	$93\frac{1}{4}°$	93°	$92\frac{3}{4}°$	90°
		γ					94°
	Cell contents Computed density		$16(NaP \cdot \frac{1}{2}H_2O)$ 1.13	$16(NaSt \cdot \frac{1}{2}H_2O)$ 1.10	$4(HP \cdot NaP)$ 1.05	$4(HSt \cdot NaSt.)$ 1.05	$6(HSt \cdot NaSt)$ 1.02
Mechanical properties	Cleavages		(001) perf. (010) perf.	(001) perf. (010) perf.	(001) perf. (010) perf.	(001) perf. (010) perf.	(001) perf. (110) perf.
	Translation-gliding plane, T direction, t		(001) [010]	(001) [010]	(001) many in (001)	(001) many in (001)	(001) ?
Optical properties	Refractive indices	α	1.505	1.507	1.506	1.506	1.498
		β	1.517	1.517	1.513	1.516	1.510
		γ	1.57*	1.56*	1.57*	1.56*	1.59*
	Optical Orientation		$X=b$ $Y\approx a$ $Z\approx c$	$X=b$ $Y\approx a$ $Z\approx c$	$X=b$ $Y\approx a$ $Z\approx c$	$X=b$ $Y\approx a$ $Z\approx c$	$X\wedge b=+40°$ $Y\wedge a=+36°$ $Z\wedge c=\ 0°$
	Optic angle	2V (in crystal)	50°	49°	49°	49°	42°
		2E (in air)	80°	78°	78°	78°	66°
		dispersion	$r>v$ strong	$r>v$ marked	$r>v$ marked	$r>v$ marked	$r>v$ marked

* Computed from α, β, and V.

This is simply pressed into the powder, which rises in the cylindrical bore, forming a core. When ejected with a wire plunger, the resulting naked core forms an ideal sample. Any type of powder pattern of soap, unless the sample was exceedingly fine grained, suffers from the effects of preferred orientation due to the platy habit and the extremely plastic nature of soap crystals.

Powder patterns of the three soap types discussed in this paper are shown in Fig. 5.

It should be noted in passing that soaps (as well as other organic crystals with large cells) cannot be identified by the Dow Chemical Company scheme[8] of tabulating the three strongest lines. This is fundamentally due to the fact that the many parameters required to locate the atoms in large cells cannot be represented by three coordinates. Such a scheme can only succeed with crystals having comparatively few atoms in the cell. A number of soaps have the three strongest lines in the same positions. Further, all soaps with the same layer spacing have a sequence or orders of 001 whose locations are identical.

Packing of soap molecules. Many properties of soap crystals are obviously related either directly or ultimately to the characteristics of soap molecules. Molecules entering into the structures of soap crystals are known on chemical grounds to be composed of long paraffin chains of hydrocarbons terminating in COOH groups for the fatty acids and COONa groups for the sodium soaps, thus:

fatty acid molecule

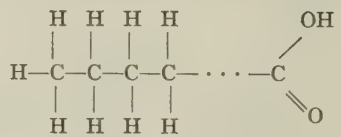

soap molecule

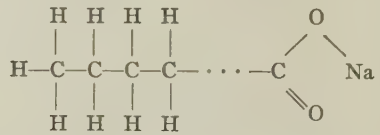

The palmitate chain contains 16 total carbon atoms, the stearate chain, 18 carbons.

The packing of such molecules to form crystals requires:

(a) that the molecules pack with long directions in parallel position in response to van der Waal's forces;

[8] Hanawalt, J. D., Rinn, H. W., and Frevel, L. K., Chemical analysis by x-ray diffraction: *Ind. and Eng. Chem.*, **80** (1938). (*Analytical Edition*, **10**, 457–512.)

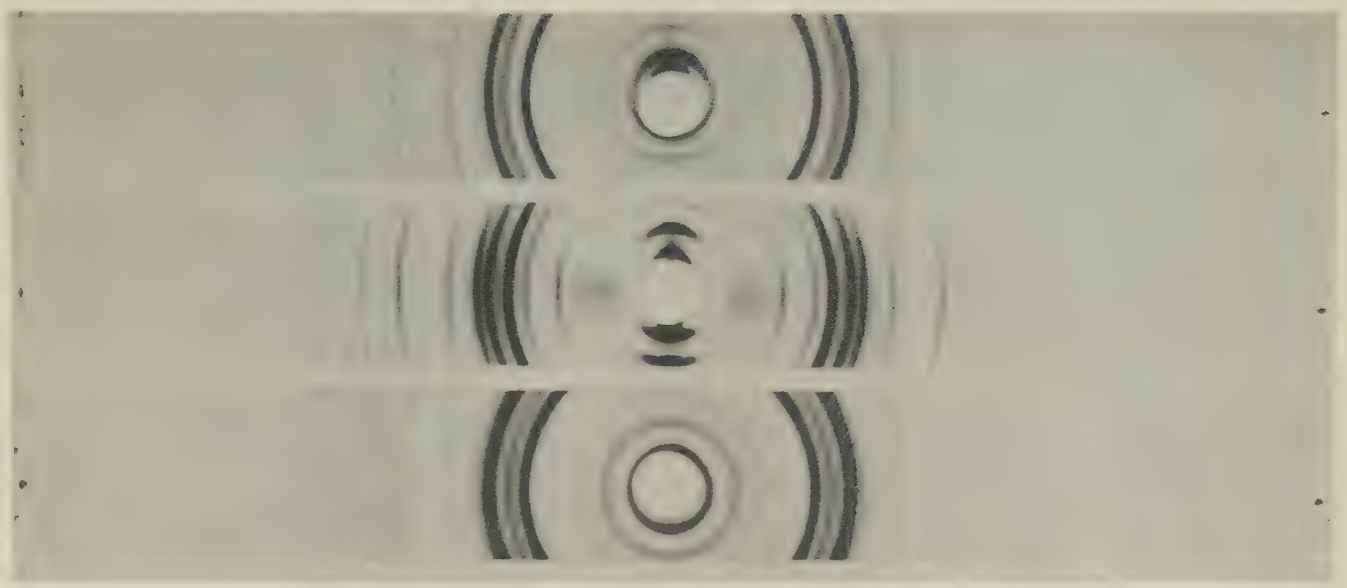

FIG. 5. *X*-ray powder photographs of representatives of the soap crystal types discussed in this paper. These photographs were taken with a camera having the standard diameter of 114.6 mm. (on which 1 mm. film distance corresponds to 1° for the deviation angle, 2θ, and to $\frac{1}{2}$° for the Bragg angle, θ). For purposes of comparison by others, these photographs are reproduced here to exactly natural size. (The middle photograph displays severe orientation which cannot be eliminated by fine-grinding the sample, since grinding causes the transformation $\alpha \rightarrow \beta$ to occur.)

Upper photograph: α NaSt.

Middle photograph: α HSt · NaSt.

Lower photograph: β HSt · NaSt.

(b) that the packing of neighboring parallel molecules be such as to distribute the positive charge concentrations of the hydrogens on the side arms of the chains;
(c) that a hydrogen bond is possible for the acid end of the acid molecule; and
(d) that the coordination requirements of the sodium in the terminations of the molecules be taken care of by an environemnt of six oxygens.

Requirements (a) and (b) are also found in crystals of paraffin molecules, whose packing has been studied by Müller.[9] Additional requirements (c) and (d) cause soap in general to utilize more complicated modes of packing than paraffins. They are also responsible for the tendency of soaps to form hydrates.[5]

Requirement (a) gives rise to the packing of soap molecules into layers, with the molecules transverse to the layers. The intermolecular forces within layers are strong while the forces between layers are comparatively weak, so that soap crystals, on heating, assume a smectic liquid crystalline condition. The layers thus act as units (transformations within layers are known, however).

Clastic and plastic properties. The layer nature of soap crystals is responsible for their most important mechanical properties. The layers can be separated, giving rise to the perfect {001} cleavages of soap crystals. They can also be slipped along one another, giving rise to the easy gliding with $T = \{001\}$. While there is a tendency toward slippage in preferred directions, as in the case of the sodium stearate and palmitate hemihydrate, this is not always discernible, and, in all cases studied, gliding can occur in any direction in the (001) plane with nearly or actually equal ease.

An x-ray study of preferred orientation in commercial soap showed that when soap is passed in heated condition past a streamlined fin, orientation results in the soap which had been in the neighborhood of the obstruction. The orientation is such that some line in (001) of the crystals tends to align itself parallel with the direction of movement of the soap past the obstruction. This is consistent with the gliding of soap layers over one another without a preferred direction in the layer.

Twinning. No twins have been observed in crystals of the α neutral soaps. Twins have been encountered in crystals of both the α and β modifications of the 1:1 acid soaps by mistaking twins for single crystals to be used in making photographs by the precession method. Studies of the precession photographs of such twins show that the twin law is reflection across (001). This implies that the crystallization of soap crystals may be attended by errors of growth in respect to the superposition of

[9] Müller, Alex. A further x-ray investigation of long chain compounds (n-hydrocarbon): *Proc. Roy. Soc.*, **120A**, 437–459 (1928).

one layer over another. This kind of error is a reasonable one to expect to occur during the growth of a layer structure.

Optical properties. The several soap crystals discussed, as well as certain crystals found in commercial soaps (as far as they can be investigated) have remarkably similar optical properties. All are biaxial positive with optic angles in the neighborhood of 45°. All have refractive indices with α and β in the neighborhood of 1.51. Optical properties thus do not constitute good criteria by which to distinguish between soap crystals.

It might be mentioned in passing that the positive optical sign is a direct consequence of the soap structure containing separated linear molecules.

BRAZILIANITE, A NEW PHOSPHATE MINERAL

FREDERICK H. POUGH, *The American Museum of Natural History*,
AND
EDWARD P. HENDERSON, *U. S. National Museum*.[1]

CONTENTS

ABSTRACT

Brazilianite is a new monoclinic phosphate mineral, $Na_2Al_6P_4O_{16}(OH)_8$. $a:b:c=1.1056:1:0.6992$; $\beta=97°22'$, $p_0'=0.6377$, $q_0'=0.6992$, $x'=0.1293$. Perfect (010) cleavage. H = 5½, S.G. = 2.94, vitreous luster, yellow-green, translucent to transparent. Biaxial +, $\alpha=1.598$, $\beta=1.605$, $\gamma=1.617$. 2V large (60–70°). Dispersion $r<v$. Occurs in large crystals in pegmatite near Cons. Pena, Minas Geraes, Brazil.

INTRODUCTION

In the course of mineralogical work in Brazil, a large yellow-green crystal was shown to F. H. Pough by a dealer who claimed it to be chrysoberyl. The symmetry and hardness at once showed that it could not be that mineral, but none was known which seemed to fit the properties. Shortly after this and a second specimen of comparable quality were acquired for The American Museum of Natural History from the owner, Sr. Oswaldo Correia of Belo Horizonte, a third crystal, identical in habit with one of the two acquired was seen at the Divisão do Geologia e Mineralogia, in Rio de Janeiro. The Curator of this collection, Dr. Evaristo P. Scorza, had received this specimen some weeks before from a mining engineer and had made a spectrographic determination of its composition in an endeavor to identify it. From the composition he assumed it to be fremontite, a very close approximation in view of his limited facilities.

[1] Published with permission of Secretary of the Smithsonian Institution.

FIG. 1. The two large brazilianite crystals of the collection of The American Museum of Natural History.

FIG. 2. 19 and 23 carat gem stones of brazilianite.

On return to this country a more extensive study was made to establish the identity of this mineral. Every one who saw these specimens was reluctant to believe it could possibly be a new mineral, yet the preliminary study of the optical and chemical properties gave this indication.

A few grains of the material were given to K. J. Murata of the U. S. Geological Survey for a spectrographic examination. He confirmed Dr. Scorza's findings that the mineral was essentially a sodium-aluminum-phosphate. The minerals fremontite and amblygonite are chemically about as closely related to the composition of the new mineral as any

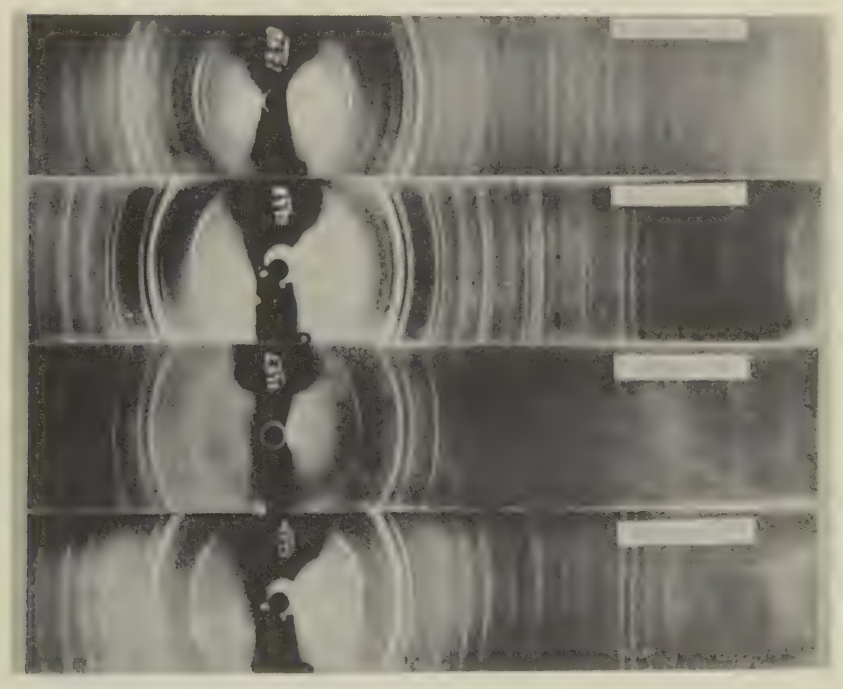

FIG. 3. *X*-ray powder photographs of allied phosphate minerals by J. M. Axelrod.

material found, assuming that the lithium of amblygonite had been replaced by sodium. In order to establish the relationship between these two minerals and brazilianite, J. M. Axelrod, also of the U. S. Geological Survey, took *x*-ray photographs of all three (Fig. 3). The photographs definitely proved that brazilianite is distinct from either of these minerals and a more detailed examination of the crystallography convinced the authors that this mineral is new to science.

Subsequently a series of additional specimens were obtained. One exceptionally large crystal weighing 973 grams was located and has been

added to the Canfield collection of minerals of the U.S. National Museum. On a second trip to Brazil, the co-author, F. H. Pough, obtained about 15 additional crystals; although much smaller, many of them were well suited for goniometric study.

The authors decided that such an important mineral should bear the name of its country of origin. Brazilite would have been our preference, but unfortunately this name had already been applied to baddeleyite, and therefore not available. Our next choice was *brazilianite*.

Crystallography

Forms. Brazilianite crystallizes in the monoclinic system. The angle-table (Table 1) shows the axial ratios and the forms noted. The calculations are based upon two-circle goniometric measurements of thirteen crystals and contact measurements upon two large crystals.

Table 1. Brazilianite Angle-Table

Monoclinic prismatic: $\frac{2}{m}$

$a:b:c=1.1056:1:0.6992$; $\beta=97°22'$; $p_0:q_0:r_0=0.6324:0.6934:1$; $r_2:p_2:q_2=1.4421:0.9122:1$; $\mu=82°38'$; $p_0'=0.6377$, $q_0'=0.6992$, $x'=0.1293$.

Forms

		ϕ	ρ	ϕ_2	ρ_2=B	C	A
c	001	90°00′	7°22′	82°38′	90°00′	0°00′	82°38′
b	010	0 00	90 00	—	0 00	90 00	90 00
a	100	90 00	90 00	0 00	90 00	82 38	0 00
β	340	34 22	90 00	0 00	34 22	85 51	55 38
m	110	42 22	90 00	0 00	42 22	85 03	47 38
i	210	55 23	90 00	0 00	55 23	83 57	34 37
h	310	69 42	90 00	0 00	69 42	83 06	20 18
j	610	79 39	90 00	0 00	79 39	82 45	10 21
n	011	10 22	35 38	82 38	55 02	67 09	83 59
z	101	90 00	37 29	52 31	90 00	30 07	52 31
x	$\bar{1}01$	−90 00	26 57	116 56	−90 00	34 19	116 56
w	$\bar{2}01$	−90 00	48 54	138 54	−90 00	56 16	138 54
v	$\bar{3}01$	−90 00	60 43	150 43	−90 00	68 05	150 43
p	113	55 43	22 28	71 08	77 34	16 53	71 36
o	111	47 25	46 10	52 31	60 47	40 59	57 55
g	$\bar{1}11$	−35 48	40 59	116 56	57 52	45 36	112 34
s	211	63 21	57 32	35 27	67 46	51 01	41 03
q	$\bar{1}21$	−19 59	56 06	116 56	38 44	58 52	106 29

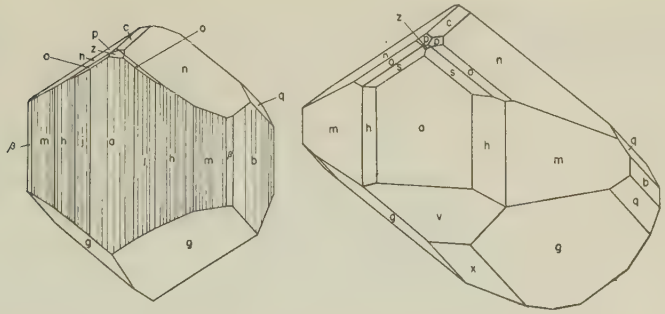

FIG. 4 (left). Brazilianite crystal of the less common slightly prismatic habit.
FIG. 5 (right). Brazilianite crystal of characteristic habit.

Habit. Crystals are of two habits, the less frequent being that shown in Fig. 4 in which the prisms are slightly elongated and so numerous in oscillatory intergrowths that the crystal is somewhat rounded in outline. One of the large crystals shows this habit as well as two of the smaller ones. Much more often we find the prism zone to be a narrow one with the attachment of the crystals at the back and the principal development in the [100] zone. Most of the smaller crystals reveal this habit and three of the larger ones, including the one at the U. S. National Museum and that of the Divisão in Rio, Fig. 5.

DISCUSSION

The prism zone is characteristically striated parallel to the *c*-axis, and all of the forms in this zone show striations. This facilitates the study of incomplete crystals; together with the cleavage the striations permit rapid orientation on the goniometer. The dominant prism is *m*, but *a* and *b*, the two pinacoids, are always present. This is well shown in the Relative Size Table[2] (Table 2) where $G_m = 55$, $G_a = 80$, and $G_b = 64$. A surprising aspect of the prism zone is the frequency of *h* (310) which is present nine out of fifteen times, with a size proportion of 53. Harmonically the prism series is not good.

The base is a relatively frequent face, as seen by its frequency index of 80, but it is always narrow and sometimes present only as a slender truncating hair's breadth form. In only one case did it show nice accessories,[3] on this crystal it was marked by a series of downward pointing symmetrical hillocks (Fig. 6), the reflections from their sides trailing off in the

[2] See Goldschmidt, V., Über Grösse und Häufiigkeit der Flächenarten: *Beiträge zur Kristal.*, **2**, 98–99 (1923).

[3] Goldschmidt, V., Über Wachstums-Gebilde: *Beiträge zur Kristal.*, **2**, 167–175 (1923).

TABLE 2. RELATIVE SIZE AND FREQUENCY STATISTICS

$H = 100 \frac{h}{n}$ H = frequency %. h = number of observations. n = number of crystals studied = 15.

$G = g \frac{100}{3n}$ G = Relative size of faces; g = 3i + 2k + l

i = occurrences as a large face
k = occurrences as a medium face
l = occurrences as a small face

FORMS	H	G	FORMS	H	G
c	80%	53%	*z*	67%	31%
b	100	64	*x*	47	22
a	100	80	*w*	6	4
β	33	22	*v*	93	55
m	100	55	*p*	53	22
i	6	4	*o*	87	40
h	60	53	*g*	100	100
j	13	11	*s*	53	29
n	100	100	*q*	53	36

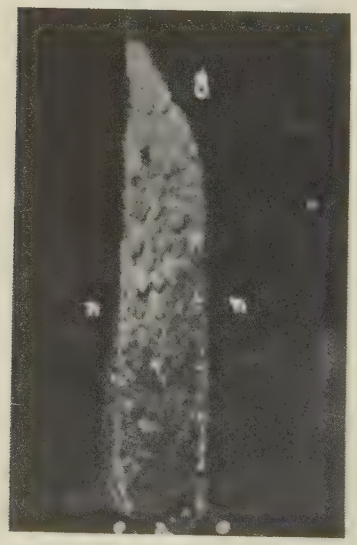

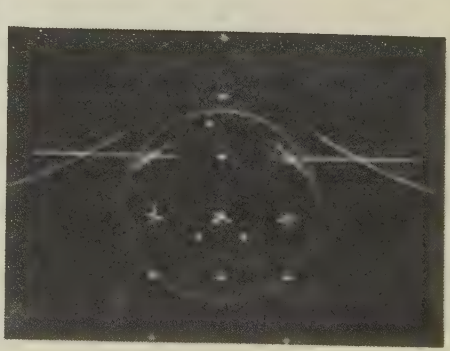

FIG. 6 (left). Growth accessories on *c*. ×9.
FIG. 7 (right). Signals and trains-of-reflection in gnomonic projection of terminal forms. 5 cm. circle base.

direction of (111) and (211) (Fig. 7). The contrasts in size and frequency, brought out by the tabulations, is well shown in the case of this form, which has a size index of 53, the same as *h*(310), though the latter has a frequency index of only 60.

The prism forms are rarely dominant on the crystals of brazilianite, usually the most prominent faces are those of the negative bipyramid *g* ($\bar{1}11$), and next in importance, the clinodome *n* (011). The surfaces of the two pairs of faces are different in detail, and it is possible to identify the forms by a study of the accessories. *n* is marked by elongated plateaus whose edges parallel the outline of the face itself (Figs. 8, 9, 10). The

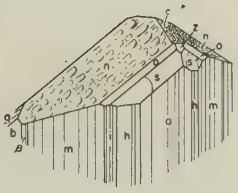

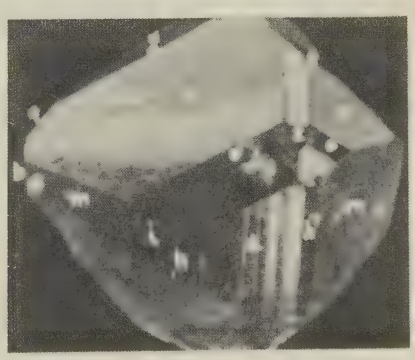

Fig. 8 (left). Characteristic growth accessories on principal faces of brazilianite.
Fig. 9 (right). Photograph of crystal in Fig. 8, showing characteristic growth accessories. ×2.

elongation is in the [100] zone. This is distinctly shown in the gnomonic projection of the trains-of-reflection from these faces (Fig. 7). The accessories, which are undoubtedly growth accessories as none of the crystals show etching phenomena of any significance, are common and were seen on most of the *n* faces; in contrast to the rarity of such irregularities on *c*. The dominant character of *n* is well shown by its size and frequency index figures, 100 and 100.

The same percentages characterize the negative bipyramid *g*. In general its appearance is similar to that of *n*, and without other forms being present it might be difficult to immediately identify these faces, were it not for the accessories, which are very different in appearance. Occasionally there are terraces shaped somewhat like those on *n*, but the elongation lies in the zone [010]. In addition, there is a frequent striation also in this direction. The truncating edges of the elongated terraces, however,

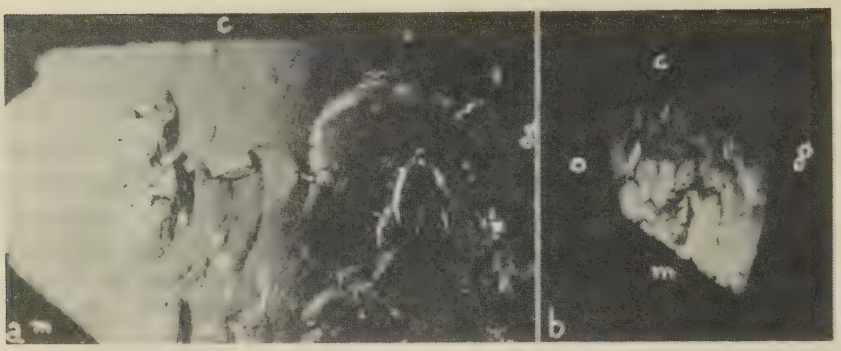

FIG. 10. Growth accessories on n (a). ×9.
(b). ×4.

cut at an angle across them, making the train-of-reflection cross, whose arms lie at about 60° to each other (Fig. 11). These sides approximately parallel the edges of the rare form w ($\bar{2}01$) and a form (021) which was not observed. The adjoining negative bipyramid q ($\bar{1}21$) is marked by a series of striations in the [010] zone and its train-of-reflections is a simple streak.

The other forms do not show any pronounced characteristic accessories, even though a number of them are relatively frequent in occurrence and large in size. The negative orthodomes x ($\bar{1}01$) and w ($\bar{2}01$) are rare, x making a slender truncation between the faces of g in about half of the crystals. w was observed but once, on the large crystal now in the U. S. National Museum collection (U.S.N.M. No. C-5797), and in this case it is a fair-sized and well developed form, but no indication of it

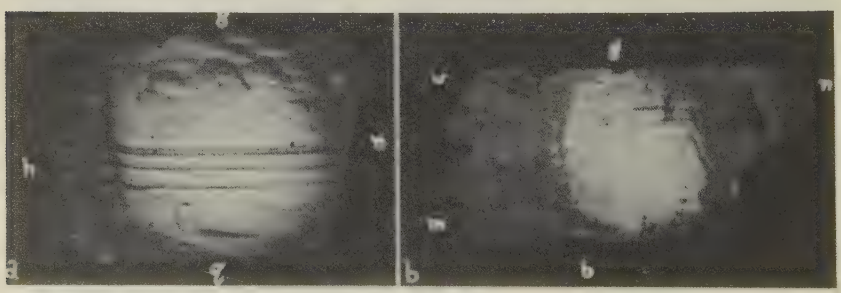

FIG. 11. Growth accessories on g (a). ×3.75.
(b). ×4.65.

was seen in any other crystal. *v*, on the other hand, is a common form, usually present and is the form which permits the proper orientation of the crystals by inspection. Its size and frequency index of 55 and 93, respectively, are indicative of its importance.

Composition

Brazilianite is distinct from any known mineral in both its physical and chemical properties. It appears to be the first reported compound of a new group of minerals, and by replacement of some of the elements in brazilianite, it may some day be expanded into quite a series of minerals.

In the following table brazilianite is compared with turquoise, chalcosiderite, and fremontite because these minerals have the closest approach in chemical composition to brazilianite. Sodium in brazilianite takes the place of the copper in the turquoise and chalcosiderite formulas and although this case is not an isomorphous series, it resembles the relationship between polyhalite and leightonite where the copper has replaced sodium in polyhalite.

Name	*Composition*					*Crystal System*
Turquoise	Cu	Al_6	P_4	O_{11}	$(OH)_{18}$	Triclinic
Chalcosiderite	Cu	Fe_6	P_4	O_{11}	$(OH)_{18}$	Triclinic
Brazilianite	Na_2	Al_6	P_4	O_{16}	$(OH)_8$	Monoclinic
Fremontite	Na_2	Al_2	P_2	O_8	$(OH)_2$, $(F)_2$	Monoclinic

Numerous tests were made to detect the presence of fluorine in brazilianite, but all gave negative results. In order to further confirm these results, K. J. Murata prepared known standards and qualitatively tested them by spectroscopic methods, and he reported no fluorine, vanadium or arsenic in brazilianite. One of the co-authors, E. P. Henderson, used the method described by J. J. Fahey for the determination of fluorine.[4]

There are many possible substitutes in the brazilianite formula and in addition to the replacement of the Na by other elements, iron may replace aluminum, and it is quite possible that vanadates and arsenates will substitute for phosphates.

Brazilianite is a hydrous sodium aluminum phosphate and its formula is: $Na_2O \cdot 3Al_2O_3 \cdot 2P_2O_5 \cdot 4H_2O$.

[4] Fahey, Joseph J., Colorimetric determination of fluorine with ferron: Analytical edition, *Industrial and Engineering Chemistry*, **11**, 362 (July 15, 1939).

Analysis of Brazilianite

E. P. Henderson, *Analyst*

		Ratios		*Theoretical composition*
Al_2O_3	43.82	.4288	3×1405	42.25
P_2O_5	37.97	.2668	2×1334	39.23
Na_2O	8.42	.1358	1×1397	8.56
K_2O	.37	.0039		
H_2O	9.65	.5356	4×1439	9.96
				100.00
Cl	trace			
F	none			
	100.23			

Physical Properties

Cleavage (010) perfect. Brittle, conchoidal fracture. H. = 5½, G. = 2.94. Luster vitreous, color chartreuse yellow, streak white. Translucent to transparent.

Optical Properties

Biaxial positive, $\alpha = 1.598$, $\beta = 1.605$, $\gamma = 1.617$. 2V large, 60–70°. Dispersion $r < v$.

Tests

Difficultly fusible, colors flame yellow. Mineral slightly expands on heating, forming a white product. Yellow color is expelled at low temperatures and the mineral becomes colorless. In closed tube brazilianite slightly decrepitates and gives off water; insoluble in hydrochloric acid.

Occurrence

It was very difficult to obtain any data regarding the exact occurrence of the mineral. It is obviously a pegmatite mineral for small crystals of muscovite are to be found all around the base of the crystals, and one or two green tourmalines may be seen included in portions of the clear crystals. White albite feldspar is associated with the muscovite in the matrix.

The locality given by Sr. Correia was not far from Arrasuahy, whereas the locality on the specimen in Rio was near Conselheira Pena, both in the State of Minas Geraes. Recently a communication from Sr. M. Pimentel de Godoy describes the source as follows: "The deposit is an altered pegmatite dike about 1 meter in width, between walls of weathered

biotite schist. The brazilianite appears to be associated with mica, feldspar and quartz. The locality is the south slope of a hill which divides the Rio Doce and the Rio São Matheus, near the head of a small tributary of the Divino River, which runs in turn into the Laranjeiras and then joins the Rio Doce. The deposit belongs to the mica group of the Conselheira Pena district, in the eastern part of the State of Minas Geraes."

Description of Specimens

Brazilianite is especially noteworthy as a new mineral because of the size and perfection of the crystals. The first two crystals obtained were of mammoth proportions. The prismatic crystal is about 85 mm. long in the direction of the *c*-axis and about 80 mm. from front to rear. It weighs 868 gms. The second, and more common type of crystal has a narrow striated prism zone, the faces themselves being only 15 to 40 mm. long, and the longest direction along the *c*-axis is only about 70 mm. Along the *a*-axis, from front to rear, on the other hand, it measures about 100 mm., and along the *b*-axis it is about 75 mm. This crystal weighs, with its mica and feldspar matrix, 852 gms. (Fig. 1).

The crystals are transparent when they are unflawed, and they include many flawless areas. The side pinacoid cleavage is pronounced and cracks are to be seen within the crystals paralleling this cleavage direction. The color appears to vary slightly; some portions of one of the crystals, however, are definitely greener than others. Other than the flaws, the only inclusions noted were some slender crystals of green tourmaline and muscovite.

Brazilianite possesses an attractive yellowish-green color, not greatly different from chrysoberyl, and when clear pieces were found it was decided to recover a gem stone. A large, clear fragment supplied by Dr. Scorza was cut by Anthony Espositer of New York City, and two large stones were obtained, one an emerald cut of 23 carats and the other a 19 carat oval brilliant (Fig. 2). The larger stone was sent to Dr. Scorza for the collection of the Divisão do Geologia e Mineralogia in Rio, and the other is in the collection of The American Museum of Natural History.

The emerald cut stone appears to have a slightly deeper green color than the oval brilliant. This may be due to the difference in orientation of the two stones with respect to the original crystal; or to the optical effect such as loss of refracted light from the sides of the stone, or perhaps to the fact that the original crystal was not absolutely uniform in color. Dichroism is slight. Mr. Espositer reported that the cutting was no more difficult than any other stone of equal hardness and that the perfect cleavage of brazilianite caused no trouble.

It is of interest to gem collectors to find a new gem stone, but it is of greater pleasure to the mineralogist who is so fortunate as to describe a new mineral of such excellent quality that it can be used as a gem stone. Brazilianite is soft and therefore will never become an outstanding or popular stone, regardless of the beauty it may possess. The refractive indices being near to 1.60 and its low dispersion indicates that brazilianite can hardly exceed yellow beryls in brilliance, and it will be less durable than beryls.

Acknowledgments

The authors acknowledge the suggestions given during this study by W. T. Schaller and M. Fleischer of the U. S. Geological Survey, in addition to those mentioned directly in the paper.

THE KNOOP MICROHARDNESS TESTER AS A MINERALOGICAL TOOL[1]

HORACE WINCHELL[2]

ABSTRACT

The Tukon testing machine with a Knoop indenter has useful possibilities in the measurement of hardness of mineral specimens. Not only does the instrument afford numerical hardness values such as argentite = 25, calcite = 100, fluorite = 150, magnetite = 700, corundum = 2000, SiC = 3000, and diamond = about 8000, but it repeats these numbers with an accuracy of between 2 and 5 per cent when applied to a given crystal face under constant conditions. Surprisingly large variations of hardness have been found in many crystals, the variation being a function of the orientation of the surface tested and of the orientation of the long axis of the Knoop indenter in that surface. The results of 479 tests in 92 different orientations on 16 different minerals and mineral-like substances indicate the instrument is worthy of further study as a mineralogical tool.

INTRODUCTION

Metallurgists have long used various types of indenters for testing the hardness (defined as resistance to deformation) of metals. Attempts to apply to minerals the Rockwell, Vickers, and other types of machines which measure hardness in terms of deformation of the specimen by penetration of a standard-shaped point applied by a specified machine, have met with little success because of the tendency of minerals to fracture during the penetration of the indenter. Since the fracture represents displacement and deformation of other material than that immediately adjacent to the point of the indenter, greater penetration takes place than is proper for the indenter and its associated machine. Moreover, the displacement due to fracture cannot be measured readily, and therefore introduces an unknown factor into the measurement. Experiments conducted at the Research Laboratories of the Hamilton Watch Company have suggested that of all the various machines for measuring hardness by indentation, the Knoop microhardness tester may be the only tool that can give valid, or at least consistent, readings of the hardness of minerals.

THE KNOOP INDENTER

Knoop, Peters, and Emerson (1939) described an unusually sensitive pyramidal-diamond indenter which is known as the microhardness tester, or Knoop indenter. The Wilson Mechanical Instrument Company manufactures a machine, the Tukon tester (Fig. 1), which utilizes this indenter. In measuring the hardness of a specimen, a polished flat sur-

[1] Contribution from the Research Engineering Division, Hamilton Watch Company, Lancaster, Pennsylvania.

[2] Research crystallographer, Hamilton Watch Company, Lancaster, Pennsylvania.

face is first prepared. The Knoop indenter is then brought into contact with this surface for 20 seconds (the minimum time found adequate to assure consistent results), with a known load. The indentation thus produced is measured with a microscope, and the hardness number I is proportional to the load divided by the area of the indentation. For relatively heavy loads—say 1 to 3 kilograms—the hardness number is essentially independent of the load. Tate (1944) showed, however, that this is not strictly true for loads of 100 grams or less; he concluded that the ap-

FIG. 1. Tukon testing machine, showing Knoop indenter and rising platform on which specimens are tested.

plied load should always be reported with the hardness number: that practice is followed here. The Tukon tester is provided with several weights corresponding to loads from 100 grams up. Our instrument is not provided with smaller loads, but slight changes could easily be made which would accomplish the purpose if necessary.

The latest model of the Tukon testing machine embodies an electro-

magnetic device for applying the load without overloading by impact between the specimen and the diamond indenter. The Hamilton instrument was rebuilt to afford that protection against shock after about half of the corundum tests reported here had been completed. The error due to impact before installation of the device is believed to be mostly the result of fractures in brittle specimens, although there must have been some decrease of the hardness number due to impact of the unguarded indenter in the old form of the instrument. The tests of a fluorite specimen (Table 2) before and after rebuilding show essentially no change in hardness number due to this modification to the instrument.

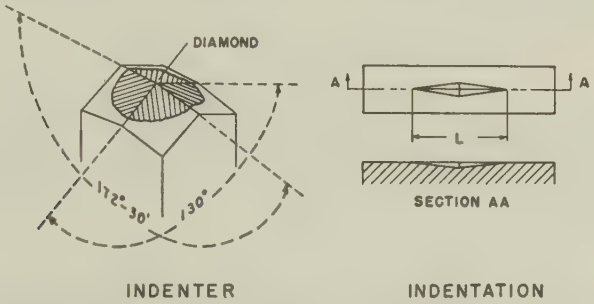

FIG. 2. Knoop indenter, showing angles between the edges of the flat pyramidal diamond point. Approximate ratios are: length:width = 7.1:1, and length:depth = 30:1.

The Knoop indenter possesses certain advantages over other similar hardness measuring tools, and these are exactly the advantages that make it suitable for testing minerals. Figure 2 shows the shape of the indenter. An extremely shallow penetration is sufficient to produce an indentation long enough to be measured with a relative accuracy of about 1%. Thus, for an indentation 100 microns (0.1 mm.) long, the penetration is only about 3 microns. The smallness of the penetrtaion was demonstrated by Peters and Knoop (1940) when they showed that a valid reading of the hardness of electrolytic chromium plate can be obtained, regardless of the nature of the base metal upon which the chromium was deposited, if the thickness of the plating is greater than 0.001 inch or 25 microns. The validity of extending this conclusion to cover small grains in a polished section of a mineral assemblage is not debated here, but does not seem unreasonable for roughly equant grains which appear about 100 microns in diameter in the plane of the section, especially if several such grains are tested and found to give consistent results. By reducing the load applied to the indenter, the length of the indentation can always be kept small.

Calculations

The conversion of the measured length of the indentation and the load on the indenter to the hardness number is made by means of the following formula, which may be expressed by a family of parallel straight lines on logarithmic graph paper:

$$I = W/L^2c$$

I = Knoop hardness number.
W = Load applied to the indenter, in kilograms.
L = Length of the indentation, originally defined as in centimeters; but L may be measured in any length units desired and the conversion factor to centimeters may be included in c.
c = a constant depending upon the shape of the indenter. It may also include conversion factors depending upon the units actually used to measure W and L.

As stated above, the equation may be expressed by straight lines, one for each applicable load, on logarithmic graph paper. The scale of the graph may be made such that there will be no danger of introducing errors that are larger than probable errors inherent in the measurement of the indentation by optical methods.

The form of the above equation shows that to achieve a given relative or percentage accuracy in I, L must be measured with a maximum relative or percentage error one-half as great. For example, if L is measured with an error of 1 part in 100, the resulting error in I would be 2 parts in 100.

Reliability

To evaluate the accuracy or consistency of the Tukon tester in the laboratories of the Hamilton Watch Company, for mineral testing purposes, several specimens were tested many times each. The results will be found summarized and expressed as probable error[3] in Table 2. It was found that most hardness readings will be repeated within about 2 to 5 per cent of the average, when many indentations are made in the same orientation on the same crystal surface. The probable error of an observation or of the average of several observations is appreciably increased if any of the observations are made on indentations associated with cracks or other fractures. In accordance with logical arguments that the highest reading will be obtained with the least fracturing, it was concluded that the *maximum* of a series of readings should be selected if fractures appear with any of them; but the *average* should be considered the best value if no fractures occurred. According to that convention, the best value is indicated in Table 2 in **boldface.**

[3] If n observations of a quantity are represented by $x_1, x_2, \cdots, x_n$, and their mean by $\bar{x}$, and their respective deviations from $\bar{x}$ by d_i, then the probable error of any individual observation is $0.6745\sqrt{\Sigma d_i^2/(n-1)}$ and the probable error of the mean is $0.6745\sqrt{\Sigma d_i^2/n(n-1)}$.

A note of caution must be included here regarding these measures of accuracy. The "probable error" shown in Table 2 and defined above is really a measure of the self-consistency of the given set of observations. It takes no account of possible systematic errors such as the dependence of the hardness number upon the load on the indenter (Tate, 1944), or imperfectly shaped or polished indenters. "Probable errors" also do not include errors due to faulty specimen preparation (polishing, levelling, etc.) or improper adjustment of the Tukon testing machine. Our efforts were mainly to control such variables by holding them constant. We have made no attempt to determine the importance of such factors for this study. Another still undetermined source of possible error is the crystallographic orientation of the diamond indenter. So far as is known, the makers of the indenters do not attempt to hold this constant. This factor would undoubtedly be negligible for soft and medium specimens but in testing materials of great hardness, the elastic properties and hardness of the diamond itself would be of the same order of magnitude as those of the specimen, and should therefore be considered. It is our impression that such properties would vary appreciably with the orientation of the diamond.

For all these reasons, then, the reader is cautioned not to accept uncritically the fourth, nor even the third significant figures of the hardness numbers quoted in Table 2. The probable error alone (2% to 5%) would generally indicate that the fourth digit can have little significance. Nevertheless, until full information on validity of results is available from all sources, it seems best not to round off the numbers farther than to the nearest 5 units in the fourth significant figure. This consideration probably would not affect results for soft materials, but might noticeably affect those reported for materials of greater hardness than 1000.

Specification of Orientation

To correlate hardness numbers with orientation of the test surface and of the long axis of the indenter in that surface, three independent coordinate angles are necessary. These angles may be compared with longitude, colatitude, and azimuth or bearing on the surface of the earth. The two-circle goniometer studies of Goldschmidt, Palache, and others (Dana-Palache et al. 1944, pp. 3–37) form the basis for the definition of the orientation coordinates of the surface tested:

"longitude" = phi (ϕ)
"colatitude" or polar distance = rho (ρ).

The azimuth or bearing, designated theta (θ), is measured clockwise from the north or meridian direction to the long axis of the indenter. Figure 3 shows these angles in stereographic projection. Phi (ϕ) is measured

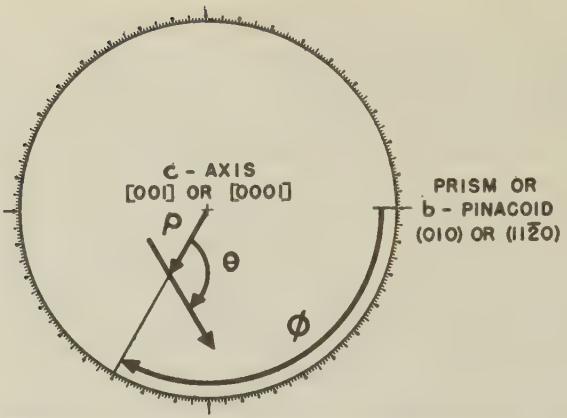

FIG. 3. Stereographic projection illustrating the definitions of ϕ, ρ, θ, the angular coordinates of the test surface and of the long axis of the indentation therein, taken with respect to conventional crystal axes of any system. For the orientation $\rho = 0°$, ϕ is indeterminate and θ is specially defined as the direction-angle, measured around the fundamental circle normally used for ϕ.

clockwise about the fundamental circle of the projection from the point representing the plane (010) or (11$\bar{2}$0). Rho (ρ) is the polar angle, measured radially outward from the center of the projection (the point representing the axis of the prism zone). And theta (θ) is measured clockwise about the point representing the test plane. These definitions serve for all points except the pole of the sphere ($\rho = 0°$). At this point, θ must be defined specially, as the direction-angle measured like ϕ around the fundamental circle.

It will be evident that these definitions permit choosing the following ranges for the three coordinate angles:

$$-180° < \phi \leqq 180°$$
$$0° \leqq \rho \leqq 180°$$
$$0° \leqq \theta < 360°$$

However, ϕ and ρ may be limited to smaller values by taking into consideration the symmetry of the applicable crystal class, as shown in Table 1. Also θ may be limited to smaller values by the twofold symmetry axis of the indenter itself, and also to special values if the test plane is normal to certain symmetry planes or to an axis of higher symmetry in the crystal. In general, $0° \leqq \theta < 180°$, because of the symmetry of the indenter only.

Graphical calculations leading to the expression of the coordinates are not difficult for most crystals. They are most easily carried out by means of gnomonic or stereographic projections based upon Laue back-reflection

TABLE 1. LIMITS OF VARIATION OF ϕ AND ρ RESULTING FROM CRYSTAL SYMMETRY

Symmetry Class				ϕ		ρ	
Symbol			Name	From	To	From	To
Isometric System							
4/m	$\bar{3}$	2/m	Normal	0	45	0	55
4	3	2	Plagiohedral	0	90	0	55
$\bar{4}$	3	m	Tetrahedral	0	45	0	55
2/m	$\bar{3}$		Pyritohedral	0	90	0	55
2	3		Tetartohedral	−90	90	0	55
Hexagonal System							
6/m	2/m	2/m	Normal	0	30	0	90
6	2	2	Trapezohedral	0	60	0	90
6	m	m	Hemimorphic	0	30	0	180
$\bar{6}$	m	2	Trigonal	−30	30	0	90
6/m			Tripyramidal	0	60	0	90
6			Pyramidal-Hemimorphic	0	60	0	180
$\bar{6}$			Trigonal-Tetartohedral	−60	60	0	90
$\bar{3}$	2/m		Rhombohedral	−30	30	0	90
3	2		Trapezohedral	0	60	0	90
3	m		Rhombohedral-Hemimorphic	−30	30	0	180
$\bar{3}$			Tri-Rhombohedral	−60	60	0	90
3			Trigonal-Tetartohedral-Hemimorphic	−60	60	0	180
Tetragonal System							
4/m	2/m	2/m	Normal	0	45	0	90
4	2	2	Trapezohedral	−45	45	0	90
4	m	m	Hemimorphic	0	45	0	180
$\bar{4}$	2	m	Sphenoidal	−45	45	0	90
4/m			Tripyramidal	0	90	0	90
$\bar{4}$			Tetartohedral	−90	90	0	90
4			Pyramidal-Hemimorphic	0	90	0	180
Orthorhombic System							
2/m	2/m	2/m	Normal	0	90	0	90
2	2	2	Sphenoidal	−90	90	0	90
2	m	m	Hemimorphic	0	90	0	180
Monoclinic System							
2/m			Normal	−90	90	0	90
2			Hemimorphic	−180	180	0	90
m			Clinohedral	−90	90	0	180
Triclinic System							

TABLE 2. KNOOP HARDNESS AS A FUNCTION OF ORIENTATION IN CERTAIN MINERALS

Substance Tested (Tests conducted on polished artificial surfaces unless otherwise noted.)	Orientation					No. Observations	Load (Kilograms)	Hardness			Probable Error (2)	Fractures (2)
	Angular Coordinates (1)			Surface (hkl) or (hkil)	Direction [hkl] or [hkil]			Minimum	Maximum (2)	Average (2)		
	ϕ	ρ	θ									
Beta Alumina,												
crystal surface	22	2		0001		3	.1	1025	**1090**	1055	**26**	x
Argentite						4	.1	24	26	**25**	**1**	
Calcite,												
cleavage surface	30	45	0	$10\bar{1}1$	$\bar{1}012$	5	.1	111	**122**	116		x
same surface			38	$10\bar{1}1$	$01\bar{1}1$	5	.1	84	**118**	99		x
same surface			90	$10\bar{1}1$	$\bar{1}2\bar{1}0$	5	.1	64	**85**	75		x
Corundum, synthetic												
Colorless block	27	89	0	$10\bar{1}0$	0001	3	.1	2065	2135	**2110**	**16**	
same surface			47	$10\bar{1}0$		3	.1	2135	2210	**2185**	**17**	
same surface			90	$10\bar{1}0$	$\bar{1}2\bar{1}0$	3	.1	2100	**2175**	2135	**25**	x
same surface			130	$10\bar{1}0$		3	.1	1900	1960	**1940**	**14**	
Colorless block	8	89	47	$11\bar{2}0$		3	.1	2065	**2135**	2100	**25**	x
same surface			90	$11\bar{2}0$	$\bar{1}100$	3	.1	1995	**2065**	2030	**23**	x
same surface			133	$11\bar{2}0$		3	.1	2175	2335	**2240**	**23**	
same surface			179	$11\bar{2}0$	0001	2	.1	1900	2030	**1965**	**44**	
Colorless block	—	2	0	0001	$11\bar{2}0$	3	.1	1960	**1995**	1985	**13**	x
same surface			30	0001	$10\bar{1}0$	3	.1	1725	**1930**	1850	**75**	x
same surface (3)			var	0001	var	31	.1	1865	**2210**	2050	**49**	x
selected indentations (4)			var	0001	var	18	.1	1960	2210	**2075**	**11**	
selected indentations (5)			var	0001	var	13	.1	1865	**2100**	2015	**53**	x
Light ruby block	27	88	0	$10\bar{1}0$	0001	3	.1	2065	2135	**2085**	**16**	
same surface			47	$10\bar{1}0$		3	.1	2135	2210	**2175**	**15**	
same surface			90	$10\bar{1}0$	$\bar{1}2\bar{1}0$	3	.1	1960	2100	**2040**	**28**	
same surface			130	$10\bar{1}0$		3	.1	2250	2420	**2310**	**36**	
Light ruby block	−1	88	0	$11\bar{2}0$	0001	3	.1	2065	2250	**2175**	**39**	
same surface			36	$11\bar{2}0$		3	.1	1900	2065	**1985**	**32**	
same surface			92	$11\bar{2}0$	$\bar{1}100$	3	.1	1670	**1900**	1765	**76**	x
same surface			144	$11\bar{2}0$		3	.1	1750	1900	**1840**	**30**	
Light ruby block	8	5	26	0001	$10\bar{1}0$	3	.1	1835	2065	**1935**	**45**	
same surface			112	0001	$\bar{1}2\bar{1}0$	3	.1	1810	1960	**1900**	**31**	
Light ruby slab	14	4	35	0001		5	.3	1510	**1630**	1560		x
same surface			80	0001	$1\bar{1}00$	5	.3	1355	**1535**	1435		x
same surface			128	0001		5	.3	1365	**1535**	1420		x
same surface			171	0001	$\bar{1}\bar{1}20$	5	.3	1265	**1425**	1350		x
Light ruby slab	−20	46	42			5	.3	1645	**1720**	1690		x
same surface			83			5	.3	1525	**1720**	1640		x
same surface			133			5	.3	1815	1870	**1850**		
same surface			179			5	.3	1765	1800	**1785**		
Light ruby slab	14	53	43			5	.3	1645	**1815**	1770		x
same surface			88			5	.3	1600	**1705**	1650		x
same surface			142			5	.3	1765	1850	**1800**		
same surface			175			5	.3	1785	1850	**1830**		
Light ruby slab (6)	−28	58	var			81	.3	1160	**1905**	1725	**79**	x
same surface			2			28	.3	1615	1785	**1705**	**5**	
same surface			40			23	.3	1765	**1905**	1850	**28**	x
same surface			95			12	.3	1470	**1765**	1660	**77**	x
same surface			129			9	.3	1160	**1720**	1570	**115**	x
Light ruby rod	28	63	63			4	.1	1780	**1835**	1815		x
same surface			154			4	.1	2100	2210	**2145**		

TABLE 2. KNOOP HARDNESS AS A FUNCTION OF ORIENTATION IN CERTAIN MINERALS—*Cont.*

Substance Tested (Tests conducted on polished artificial surfaces unless otherwise noted.)	Orientation					No. Observations	Load (kilograms)	Hardness			Probable Error (2)	Fractures (2)
	Angular Coordinates (1)			Surface (hkl) or (hkil)	Direction [hkl] or [hkil]			Minimum	Maximum (2)	Average (2)		
	ϕ	ρ	θ									
Light ruby rod	28	75	69			4	.1	1900	**1960**	1930		x
same surface			159			4	.1	1995	2065	**2030**		
Light ruby rod	−24	53	42			4	.1	1995	2100	**2045**		
same surface			129			4	.1	2030	**2100**	2055		x
Dark ruby slab	0	66	45			5	.3	1675	**1850**	1755		x
same surface			86			5	.3	1660	**1750**	1725		x
same surface			130			5	.3	1940	1975	**1955**		
same surface			178			5	.3	1735	1815	**1780**		
Fluorite	42	53	0	111	$\bar{1}\bar{1}2$	3	.1	137	141	**139**	1	
repeat run (10)						8	.1	142	155	**148**	1	
same surface			30	111	$\bar{1}01$	3	.1	143	157	**152**	4	
repeat run (10)						8	.1	144	158	**155**	1	
Galena (7)		1	0	001	010	4	.1	66	79	**71**	4	?
same surface			45	001	110	4	.1	62	74	**67**	4	?
Galena (7)	45	53	0	111	$\bar{1}\bar{1}2$	5	.1	53	69	**60**	4	?
same surface			30	111	$\bar{1}01$	5	.1	55	65	**59**	3	?
Glass												
Micro slide						7	.1	438	507	**478**		
Cover glass						5	.1	482	494	**489**		
High-alumina glass for jewel bearings												
Fire polished							.5	542	553	**548**		
Mechanically polished							.5	546	557	**551**		
Gypsum,												
cleavage surface	0	90	0	010	001		.1		(8)			x
same surface			81	010	100	3	.1	43	**46**	44	2	x
same surface			115	010	$\bar{1}0\bar{1}$	3	.1	33	**54**	40	10	x
Kyanite	40	5	36	001	100	5	.1	1175	**1255**	1205		x
same surface			126	001	010	6	.1	165	**205**	184		x
Kyanite	12	91	0	010	001	6	.1	1035	**1420**	1260		x
same surface			90	010	100	6	.1	1645	**1695**	1665		x
Kyanite	70	90	0	100	001	5	.1	933	**1325**	1120		x
same surface			90	100	010	5	.1	360	**520**	462		x
Magnetite	10	25	(?)			4	.1	735	782	**761**	8	
Magnetite	45	35	(?)			4	.1	611	623	**618**	2	
Quartz, crystal face	30	52	0	$10\bar{1}1$	$\bar{1}012$	3	.1	640	685	**666**	11	
same surface			48	$10\bar{1}1$	$0\bar{1}11$	3	.1	728	766	**748**	9	
same surface			90	$10\bar{1}1$	$\bar{1}2\bar{1}0$	3	.1	628	**653**	640	8	x
Quartz, crystal face	−30	52	0	$01\bar{1}1$	$0\bar{1}12$	3	.1	679	**720**	699	14	x
same surface			43	$01\bar{1}1$	$\bar{1}011$	3	.1	728	766	**748**	9	
same surface			90	$01\bar{1}1$	$2\bar{1}\bar{1}0$	3	.1	665	685	**674**	5	
Quartz, crystal face	30	90	2	$10\bar{1}0$	0001	3	.1	872	922	**902**	10	
same surface			50	$10\bar{1}0$	$\bar{2}4\bar{2}3$	3	.1	808	816	**811**	2	
same surface			87	$10\bar{1}0$	$\bar{1}2\bar{1}0$	3	.1	774	**834**	797	22	x
Silicon carbide (9)												
Black, crystal face (9)		0	0	0001	$11\bar{2}0$	10	.1	2760	3220	**3010**	60	
same surface			15	0001		10	.1	2620	3000	**2855**	60	
same surface			30	0001	$10\bar{1}0$	10	.1	2800	3225	**3010**	60	
same surface, average		0		0001	var	30	.1	2620	3225	**2960**		

TABLE 2. KNOOP HARDNESS AS A FUNCTION OF ORIENTATION IN CERTAIN MINERALS—*Cont.*

Substance Tested (Tests conducted on polished artificial surfaces unless otherwise noted.)	Orientation: Angular Coordinates (1) ϕ	ρ	θ	Surface (hkil) or (hkil)	Direction [hkl] or [hkil]	No. Observations	Load (Kilograms)	Hardness: Minimum	Maximum (2)	Average (2)	Probable Error (2)	Fractures (2)
Green, crystal face (9)		0	0	0001	$11\bar{2}0$	10	.1	2650	2800	**2740**	**60**	
same surface			15	0001		10	.1	2430	2920	**2675**	**60**	
same surface			30	0001	$10\bar{1}0$	10	.1	2690	3000	**2830**	**60**	
same surface, average		0		0001	var	30	.1	2430	3000	**2740**		
Sphalerite	6	42	(?)			3	.1	175	180	**177**	**2**	
Spinel, synthetic blue	40	30	63			3	.3	1200	**1235**	1225	**15**	x
same surface			123			3	.3	1105	**1165**	1135	**20**	x
same surface			177			3	.3	1080	**1115**	1100	**11**	x
Topaz, cleavage surface		0	0	001	010	5	.1	846	**1040**	960		x
same surface			45	001		5	.1	889	**1160**	1060		x
same surface			90	001	100	5	.1	769	**985**	894		x
same surface			−45	001		5	.1	1160	**1230**	1215		x

NOTES TO TABLE 2

(1) Angular coordinates are as defined in Fig. 3 and as measured by means of x-ray diffraction patterns.
(2) In the column headed *Fractures* is indicated the presence of small fractures observed about the marks of the indenter. If fractures were present, the *maximum* hardness reading of a series is considered the best, and is so indicated by **boldface** numerals, but if no fractures were observed, the *average* is considered the best value obtainable from the series, and is so indicated by the same means. The *probable errors* were calculated for the maximum or for the average, whichever is considered best value.
(3) Indentations in 31 different directions.
(4) Selected indentations with no fractures.
(5) Selected indentations with minor fractures.
(6) Combined results from the following four items.
(7) No fractures visible, but fractures probable on account of the excellent cleavage.
(8) Large fractures; measurements impossible at lightest available loads (.1 Kg).
(9) Probable errors for silicon carbide observations are approximate.
(10) Original measurements August, 1942. Repeated January, 1945, because of question raised by comparison with published results (Table 3), and to observe effect of addition of magnetic device for preventing indenter-overload due to impact.

x-ray patterns made with the test plane parallel with the x-ray film and normal to the x-ray beam. The position of the long axis of the indentation must be noted with respect to the top or other mark on the x-ray film at the time of setting up for the diffraction pattern; otherwise θ may be lost. In hexagonal and tetragonal crystals, the extinction angle may be measured by polarized light to determine θ, provided the specimen is transparent and in a suitable mounting.

RESULTS OF TESTS

Table 2 contains the collected results of mineral hardness determinations made at the Hamilton Watch Company laboratories over a period of approximately 3 years. Bearing in mind the rather academic importance of most of these results, the reader will understand why more ex-

tensive tests cannot easily be made here. This list does include a wide enough variety of minerals and mineral-like materials to indicate very promising possibilities for application of the Knoop indenter to determinative mineralogy and to crystallography. Several type-minerals in Mohs' scale, and some in the scale of hardness of Talmage (1925), are included in Table 2. It should be emphasized that determinations from fractured indentations marked "x" were of a reduced order of accuracy because of the fractures. Such determinations should not be considered final nor necessarily even approximately accurate; they are the best we have available, however, and it will be noted that even in spite of the uncertainty introduced by the presence of fractures, the fractures themselves appear to have been fairly consistent for any given orientation, and the readings therefore were fairly constant. Analysis of the table will show that the largest probable error for a good determination is less than 5% of the hardness number.

It is especially to be noted that most of the substances tested in several orientations showed *considerable variations of hardness with orientation*. The well-known variation of scratch-hardness with scratch direction on the macropinacoid of kyanite is reflected by variations obtained by indenting that surface with the indenter either parallel to, or at right angles to the direction of the *c*-axis. If we consider the direction of scratching and the azimuth of the indenter for the highest hardness value observed on the surface tested, we note a discrepancy as follows:

Azimuth (θ) for maximum hardness in kyanite

Test Surface	Method of Test	
	Indenter	Scratch
(001)	about 36°	same
(100)	0°	90°

No explanation of this apparent anomaly can be offered here. It may be due to the excellent cleavage of the mineral, and it may be due in part to the fractures that were produced in the material by the indenter.

Comparison with Results of Others

So far, only a few investigators have reported any findings regarding the applicability of the Knoop microhardness tester to mineral specimens. Knoop, Peters, and Emerson (1939), and Peters and Knoop (1940) published a few mineral hardness tests in their early descriptions of the instrument. Table 3 shows the mineral hardness values quoted by them,

Table 3. Comparison of Knoop Microhardness Numbers

Mineral	Knoop et al. (1939)	Peters et al. (1940)	Winchell (1945)
Gypsum	32	32	46–54*
Calcite	135	135	75–120*
Fluorite	163		139–152*
Apatite	360–493*		
Albite	490		
Orthoclase	560		
Quartz	710–790*	710–790*	666–902*
Topaz	1250		1040†
Alundum	1635	1620–1635	
Synthetic corundum			1700–2200*
Black SiC		2050–2150	2850–3000
Green SiC		2130–2140	2675–2825
Diamond	8000–8500	8000–8500	

* Variation due at least in part to orientation of different test surfaces and/or different positions of indenter therein.

† Topaz determinations at Hamilton probably low on account of fractures.

together with results obtained here. Our results (Table 2) suggest that the ranges indicated are real, and may be due to the variations of hardness with crystallographic orientation: since they do not represent a complete exploration of all orientations, it is likely that they should be even wider than indicated. Differences between our results and those of the Bureau of Standards appear to be real, possibly instrumental differences, but they are probably due in part to orientation differences. Some differences may be due also to the use of indentations with small fractures.

Acknowledgment

Grateful acknowledgment is due the Hamilton Watch Company for support of this work, and for the use of the Tukon tester. Special credit is due Mr. G. E. Shubrooks, Chief Chemist and Metallurgist, and Mr. J. H. Swarr, Metallurgist, for their cooperation and interest in the project. Mr. Swarr conducted or supervised nearly all the tests reported here, often under conditions made difficult by the tendency of the minerals to fracture excessively under all but the lightest loads. The Wilson Mechanical Instrument Company, New York, kindly furnished the photograph of the Tukon Tester which is reproduced as Fig. 1.

The critical comments of Dr. N. W. Thibault of Norton Company, Worcester, are hereby acknowledged. Dr. Thibault's reading and criticism of the manuscript has led to clarification of several points that

otherwise could easily have been misunderstood. Statements of fact or opinion, however, are the writer's, and do not necessarily reflect Dr. Thibault's views.

Conclusion

The Knoop microhardness tester, embodied in the Tukon testing machine, is a new mineralogical tool which appears to deserve further investigation. This tool is apparently capable of detecting and measuring variations in hardness on different crystal faces of corundum, magnetite, calcite, and other materials. It shows some unexplained anomalies when applied to kyanite, which is a mineral noted for its hardness variations. Kyanite shows hardnesses ranging from 205 to 1700, depending upon the orientation of the test surface, and of the long axis of the Knoop indenter in that surface. The Knoop hardness of gypsum is approximately 32 to 45 or more, depending upon orientation; that of calcite is 75 to 135; that of fluorite, 140 to 150; of orthoclase, 560; of quartz, 666 to 900; of topaz, 1250; of corundum, 1700 to 2200; and of diamond, about 8000. The instrument reproduces its own results within an accuracy of 2% to 5%, depending upon the hardness and brittleness of the specimen, and such accuracy can be achieved in testing grains only 100 microns in diameter in polished sections.

Bibliography

Brodie, Constance B. (1944), The microhardness tester as a metallurgical tool: *Trans., Am. Soc. Metals*, **33**, 126.

Dana-Palache et al. (1944), *Dana's System of Mineralogy, Part I*, by C. Palache, H. Berman, and C. Frondel. New York, (**1944**).

Knoop, F., Peters, C. G., and Emerson, W. B. (1939), Sensitive pyramidal-diamond tool for indentation measurements: *U. S. National Bureau of Standards*, Research Paper No **RP1220**; the Bureau's *Journal of Research*, **23**, July, 1939, 39–61.

Peters, C. G., and Knoop, F. (1940), Metals in thin layers—Their microhardness: *Metals and Alloys*, **13**, 292.

Talmage, S. B. (1925), Quantitative standards for hardness of the ore minerals: *Econ. Geol.*, **20**, 531–553.

Tate, D. R. (1944), A comparison of microhardness tests: *Trans., Am. Soc. Metals* (1944 Preprint 1, available from Society headquarters).

COMPOSITION OF THE BIRD RIVER CHROMITE, MANITOBA*

J. D. Bateman**

Abstract

Analyses of the Bird River chromite indicate an excess of ferric oxide in the lower grade ores, which is verified by the presence of exolved hematite in the chromite crystals. Similar hematite inclusions in the higher grade ores are not indicated by recasts of the analyses, suggesting that some of the bivalent oxides (after excluding silicate gangue and ilmenite) do not enter into the chromite molecule.

Introduction

Large deposits of chromite were discovered during 1942 in the Lac du Bonnet district of Manitoba about 80 miles northeast of Winnipeg. The geology and details of occurrence of the chromite have been described[1] and are briefly summarized here.

Stratiform chromite deposits occur in a composite basic sill of early pre-Cambrian age that has been folded into an easterly plunging anticline north of Bird River. The sill is from 500 to 3500 feet thick, both limbs being about vertical. It consists of two sheets: an upper layer of hornblende gabbro and a lower layer of serpentinized peridotite and pyroxenite. The two sheets are probably separate intrusions closely spaced in time.

The chrome-bearing zone is confined to the upper part of the peridotite and is within 170 feet of the overlying gabbro on either limb of the fold. The deposits consist of pseudostratified layers of dense and disseminated ores alternating with peridotite and chromiferous peridotite.[2] Some minor deposits are found as irregular lenses of chrome ore in the base of the gabbro. The principal occurrences consist of 5 or more chrome-bearing layers.

None of the chromite is massive, and the dense ores consist of close-packed small (up to 0.5 mm.) octahedral chromite crystals in a gangue of chlorite and tremolite with pyroxene residuals. Such ores contain from 20 to 30 per cent chromic oxide. In the disseminated ores, which carry from 12 to 20 per cent chromic oxide, the chromite is interstitial to the gangue. The boundaries between the dense and disseminated ores are normally sharp.

* Published with the permission of the Director, Mines and Geology Branch, Department of Mines and Resources, Ottawa.

** Geological Survey, Ottawa.

[1] Bateman, J. D., *Trans. Can. Inst. Min. Met.*, **46**, 154–183 (1943).

[2] The peridotite is a pyroxene-rich variety with relatively little olivine, the original ferromagnesian minerals being largely altered to chlorite and serpentine.

FIG. 1. Photograph showing banded character of chromite (dark layers). Oblique lines on right side of picture are glacial striae.

The main chrome deposits, which are from 6 to 12 feet wide and several thousands of feet long, contain from 18 to 26 per cent chromic oxide. This ore can be raised by table concentration to a grade of 35 to 42 per cent chromic oxide, the product having a chrome-iron ratio between 1.2:1 and 1.5:1.

The deposits are believed to have originated as magmatic segregations of chrome ore resulting from crystal sedimentation during cooling of the lower part of the Bird River sill. Late magmatic or deuteric hydrothermal action effected some mineralogical modifications, particularly of the gangue.

COMPOSITION OF THE CHROMITE

The samples selected for analysis were ground to minus 60 mesh and concentrated on a superpanner at the Bureau of Mines. This method was found to yield a cleaner concentrate than heavy liquid separation. The samples were analyzed by R. J. C. Fabry, Chemist, Geological Survey. Ferrous and ferric oxides were not determined as such, but were calculated from total iron. The method used by Mr. Fabry is indicated in the following calculation of ferric and ferrous iron for sample No. 5:

	Al_2O_3	Cr_2O_3	MgO	FeO		
	12.65	40.26	3.79	39.32	Per cent	
	12.38	26.48	9.41	54.76	Molecular ratios	
Trivalent:	Al_2O_3	12.38		Bivalent:	MgO	9.41
	Cr_2O_3	26.48			FeO	29.45
		38.86				38.86

Excess of FeO is $54.76-29.45=25.31$

$$25.31 \Big/ \left(\frac{(FeO \cdot Fe_2O_3)}{3}\right) = 8.43\ Fe_3O_4$$

8.43×160 (M.W. of Fe_2O_3) $= 13.49$ per cent $Fe_2O_3 = 12.14$ FeO
FeO in sample is then $39.32-12.14=27.18$ per cent
$Fe_2O_3 = 13.49$ per cent

The analyses of the samples are as follows:

CLEANED CHROMITE CONCENTRATES

	(1)	(2)	(3)	(4*a*)	(4*b*)	(5)	(6)
Cr_2O_3	43.50	42.56	40.27	41.70	41.50	40.26	39.60
Al_2O_3	17.23	13.45	11.42	8.85	9.35	12.65	13.56
Fe_2O_3	8.16	7.20	16.11	15.80	21.73	13.49	13.46
FeO	20.86	24.24	20.36	27.11	21.94	27.18	30.04
MgO	8.70	8.86	7.29	3.32	3.51	3.79	2.26
CaO	0.10	0.17	0.34	0.34	0.28	0.27	0.29
MnO	0.23	0.28	0.04	0.10	0.05	0.13	0.14
TiO_2	0.39	1.81	0.37	0.84	1.30	0.44	0.62
NiO	0.02	nil	0.11	0.32	0.02	0.09	0.08
SiO_2	0.30	0.20	2.31	0.24	nil	0.12	0.08
H_2O	0.90	0.76	2.08	0.76	0.95	0.98	0.80
	100.39	99.53	100.70	99.37	100.63	99.40	100.93
Cr:Fe	1.36:1	1.23:1	1.01:1	0.88:1	0.88:1	0.90:1	0.83:1

(1) Dense black ore from layer No. 3, Chrome deposit.
(2) Dense black ore, Page deposit.
(3) Disseminated ore, layer No. 4, Chrome deposit.
(4) Disseminated ore, layer No. 4, Page deposit.†
  (4*a*) magnetic portion
  (4*b*) non-magnetic portion
(5) Dense ore in gabbro, Mayville claim, north limb of sill.
(6) Dense ore in gabbro, Wards claim, south limb of sill, west end.

† The chromite concentrates contain 1 per cent or less magnetite. In all the samples, except No. 4, all the chromite is slightly magnetic and adheres to an electro-magnet. Approximately half of sample No. 4 was non-magnetic and the two fractions were analyzed separately.

A recast of the analyses of samples 1 to 6 is shown below. The titanium oxide is calculated as ilmenite, and the gangue is indicated as a chlorite near the composition of amesite, to which all the H_2O is added.

RECAST OF ANALYSES

	(1)	(2)	(3)	(4)*a*	(4)*b*	(5)	(6)
$Cr_2O_3 \cdot$ (Fe, Mg)O	62.58	62.48	57.81	61.30	61.10	59.60	58.20
$Al_2O_3 \cdot MgO$	23.28	18.36	10.51	11.64	13.06	18.14	20.06
$Fe_2O_3 \cdot FeO$	11.83	10.44	12.53	22.97	3.71	19.49	19.49
Fe_2O_3 excess	nil	nil	7.50	nil	19.20	nil	nil
ilmenite	0.76	3.50	0.76	1.52	2.43	0.76	1.20
gangue	2.63	5.51	11.56	2.35	nil	1.46	1.67
	100.08	100.29	100.67	99.78	99.78	99.45	100.62

For purposes of comparison the chromite constituents only are shown below.

RECALCULATION OF CHROMITE CONSTITUENTS

	(1)	(2)	(3)	(4*a*)	(4*b*)	(5)	(6)
$Cr_2O_3 \cdot$ (Fe, Mg)O	63.95	68.45	65.44	63.92	62.98	61.30	59.53
$Al_2O_3 \cdot MgO$	23.96	20.11	11.90	12.14	13.44	18.66	20.52
$Fe_2O_3 \cdot FeO$	12.09	11.44	14.18	23.94	3.81	20.04	19.95
Fe_2O_3	—	—	8.48	—	19.77	—	—
	100.00	100.00	100.00	100.00	100.00	100.00	100.00

	(1)	(2)	(3)	(4*a*)	(4*b*)	(5)	(6)
$Cr_2O_3 \cdot$ (Fe, Mg)O			71.50		78.46		
$Al_2O_3 \cdot MgO$			13.00		16.77		
$Fe_2O_3 \cdot FeO$			15.50		4.77		
Without excess Fe_2O_3			100.00		100.00		

In calculating the recasts it was found that, after the amounts necessary for the gangue were subtracted, there was an excess of magnesia over the amount required to combine with the available alumina in specimens 1 and 2, which were concentrated from dense chromite ore. But in the cleaned chromite from the disseminated ores (specimens 3 and 4) the molecular amounts of magnesia equalled those of alumina; whereas in ores from the gabbro (specimens 5 and 6) there was a deficiency of magnesia. In recasting specimen 6 a small amount of excess alumina was

added to the gangue; and for sample No. 2 a small amount of magnesia was similarly added.

Discussion

The most striking feature of the recasts of the analyses is the excess of ferric iron indicated in samples 3 and 4*b*. Examination of the chromite under reflected light with high power oil immersion lenses shows the presence of free hematite. The hematite occurs as thin, microscopic blades oriented in two directions at right-angles to one another and probably conforming to crystallographic directions of the chromite. They have been described by G. M. Brownell,[3] who attributed them to exsolution. Brownell further suggests that additional unexolved ferric oxide may remain in solid solution with the chromite. Hematite inclusions were found to be most abundant in the disseminated or lower grade ores, which may account for the lower chrome-iron ratio of these ores.[4] Similar inclusions, although less abundant, occur in much of the chromite of the dense ores and in the chromite that is found in the gabbro; but the analyses of these ores do not indicate ferric oxide in excess of that required to combine with the bivalent molecules present. As free hematite does occur in the ores the most obvious conclusion is that some of the bivalent oxides may not enter into the chromite molecule. Thus in specimens 1 and 2 some of the MgO may exist as brucite and, in specimens 5 and 6 part of the FeO may be present as a hydroxide of iron.

The chrome-iron ratio of a large number of samples, both of ore and concentrates, has been determined. In most cases the ore shows little or no improvement in chrome-iron ratio upon concentration, indicating that the iron content of the gangue is low. The inferior chrome-iron ratio of the ore thus appears, in part, due to the excess of ferric iron in the chromite crystals.

[3] *Univ. of Toronto, Geol. Ser.*, No. **48**, 101–102 (1943).

[4] Bateman, J. D., *op. cit.*, p. 174.

BASTNÄSITE*

JEWELL J. GLASS AND ROBERT G. SMALLEY, *U. S. Geological Survey, Washington, D. C.*

CONTENTS

ABSTRACT

Bastnäsite, a fluocarbonate of cerium metals $(RF)CO_3$, has been found in the fluorspar deposits in the Gallinas Mountains in central New Mexico. A spectrographic analysis of the mineral has been made; x-ray diffraction patterns have been prepared and compared with patterns of bastnäsite from other previously described localities; and the optical properties and specific gravity have been determined. Minerals associated with the bastnäsite are: barite, barytocelestite, calcite, fluorite, goethite, hematite, limonite, orthoclase, pyrite, and quartz.

Bastnäsite from Ruanda-Urundi, Belgian Congo, another new locality, is also described, together with its associated minerals.

For comparison compilations of all the available data on optical properties, chemical composition, mode of occurrence, and associated minerals are given for bastnäsite. The uniformity of optical data for bastnäsite from six localities indicates a constant chemical composition, which agrees with a conclusion arrived at from a consideration of seven chemical analyses of the mineral from various localities. The summary of data also shows that most of the known occurrences of bastnäsite are in contact metamorphic rocks.

* Published by permission of the Director, Geological Survey, United States Department of the Interior.

BASTNÄSITE FROM THE GALLINAS MOUNTAINS, LINCOLN COUNTY, NEW MEXICO

Introduction

Bastnäsite, a fluocarbonate of cerium metals, $(RF)CO_3$, a rare mineral containing about 75% oxides of the cerium group, has been found in the fluorite deposits in the Gallinas Mountains, New Mexico. Bastnäsite was first discovered at Bastnäs, Sweden,[9] more than a century ago, at the same locality where, a few years before, the examination of a new mineral, cerite, led to the discovery of the metal cerium in 1804. Since the discovery of bastnäsite in Sweden, other minor occurrences have been recorded from two places in Colorado, two in Madagascar, and one in the Ural Mountains of Russia. Bastnäsite from the Gallinas Mountains, New Mexico, was identified in the Petrographic Laboratory of the United States Geological Survey, in October, 1943, in the course of mineralogic and petrographic examinations of ore samples, as a part of cooperative investigation of strategic and critical mineral deposits by the Geological Survey and the Bureau of Mines, United States Department of the Interior.

The laboratory study of the specimens, the determination of the optical properties, and the compilation of published data on bastnäsite were made by Jewell J. Glass; and the field geology and collection of specimens are largely the contributions of Robert G. Smalley. Vincent Kelley and other geologists of the Geological Survey, and engineers of the Bureau of Mines contributed valuable field data. The spectrographic examination was made by K. J. Murata, and the *x*-ray work was done by J. M. Axelrod, both of the Geological Survey, to whom the authors are greatly indebted. The authors are also indebted to E. P. Henderson of the United States National Museum, through whose cooperation samples of specimens from other localities were secured for comparison; to Fritiof M. Fryxell of the Geological Survey for his valuable aid in translating data from original Swedish publications; to Dr. C. S. Ross and to Dr. M. Fleischer for critical reading and constructive criticism of the paper.

Location

The Gallinas Mountains comprise a small rugged area elongated northwest and southeast about 10 miles long and 5 miles wide, with a maximum elevation of nearly 9000 feet, situated in the Lincoln National Forest, and almost in the geographical center of the state of New Mexico. The northern end of the mountains is crossed east and west by the county line between Torrance and Lincoln counties. The southeastern end of the mountains in Lincoln County contains mineral deposits. In times

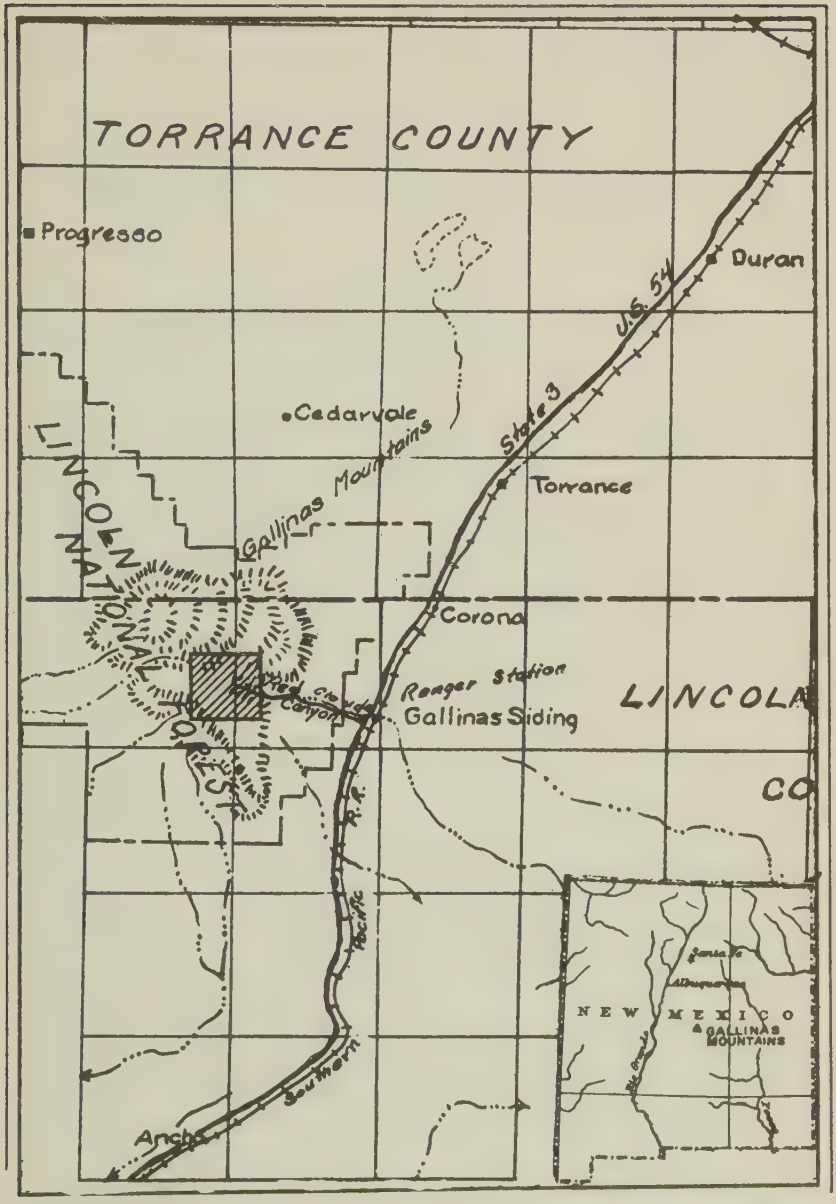

FIG. 1. Map showing the locality of the Gallinas Mountains bastnäsite deposits, Lincoln County, New Mexico.

past the region has been worked for lead and copper; and in 1943 and 1944, the area was explored by the Federal Bureaus for minable deposits of fluorspar and iron ore. The fluorspar district extends over an area of about 1 square mile in the southern part and is accessible by dirt road from the Southern Pacific R. R. and U. S. highway 54, both about eight and a half miles to the east. Carrizozo, the nearest town of any size, is 50 miles south, and Socorro is 70 miles nearly west. The region is forested but water is extremely scarce.

Occurrence

The Gallinas Mountains are characterized by a complex of igneous intrusions which have penetrated pre-Cambrian granites and overlying sediments of Permian age. The principal intrusive rocks are prophyritic quartz-monzonites, rhyolites, and syenites. They occur in large bodies which are discordant with the sedimentary rocks and irregular in outline, and as numerous small sills and dikes. A number of small lamprophyre dikes apparently belong to the same period of igneous activity. The sedimentary rocks are conglomerates, arkoses, and fine-grained sandstones interbedded with some limestones and siltstones overlying the pre-Cambrian granites. These underwent slight metamorphism previous to the igneous intrusions, and were complexly faulted and fractured during and after the intrusions.

The fluorspar deposits which contain the mineral bastnäsite occur along fissures and faults, and in fault breccias and shatter zones, usually largely within the sedimentary rocks, but most of them are near, or along the contacts of, intrusive bodies. The deposits were probably formed by ascending hydrothermal solutions which were apparently related to the igneous activity. Those which contain the largest amounts of bastnäsite occur along faults where extensive movement has taken place, resulting in wide zones of brecciated rock, and thus affording excellent channelways for the mineralizing solutions.

Bastnäsite was first found in a fluorspar deposit in the Red Cloud area, at the southern end of the mineralized district, and later it was identified as a minor constituent of the fluorspar ore in the neighboring areas—the Conqueror prospects which contain more and larger crystals of bastnäsite than most of the others, the Eagles Nest claims, the Eureka mine, and the Buckhorn mine.

The rockmass in which the bastnäsite occurs is composed largely of a purplish or brown stained, porous aggregate of interlocking crystals of barite, bastnäsite, fluorite, quartz and goethite, and hematite pseudomorphs after pyrite. Fresh crystals of bastnäsite are found wedged be-

tween altered crystals of barite, and in close association with fine-grained fluorite.

The extreme alteration of the rock in the mineralized zone indicates that it may be the result of repeated periods of hydrothermal action. Pyrite appears to have been deposited at the same time as the barite and older fluorite, at one of the earlier periods of deposition; and at a later period the entire zone was invaded by magmatic emanations rich in fluorine, carbon dioxide, and rare earths, at which time a new generation of fluorite and the bastnäsite were deposited. Bastnäsite appears to have been one of the last minerals to be deposited, and shows no evidence of having been derived from the alteration of a preexisting mineral.

Physical and Optical Properties

Bastnäsite from the Gallinas Mountains occurs in thin, tabular, hexagonal crystals usually about 4 millimeters across, although some crystals are 6 millimeters across, and seldom more than 1 or 2 millimeters thick. Clusters of platy crystals are common; some of the clusters or aggregates are 30 millimeters across. The bastnäsite crystals have a distinctly lamellar structure, each one built up of thin plates stacked one on top of the other, with edges rough and striated horizontally, similar to mica crystals. Prism faces on these thin crystals are narrow bands, or, on some crystals nearly entirely lacking, but pyramid faces are conspicuous.

Cleavage is perfect parallel to $c(0001)$. The thin laminae can be split apart with ease. The bond between the laminae apparently becomes weaker with weathering and planes of separation, or what has been called basal parting, develop. Prismatic cleavage is poor and rarely observed. Fracture uneven. Brittle. H. = 4.5, scratches fluorite but can be scratched by glass. Sp. Gr. = 4.99. Luster vitreous, sometimes resinous or waxy. Color honey yellow. Transparent to subtranslucent. Streak colorless. Infusible. Soluble in strong sulphuric acid with effervescence (CO_2) and evolution of hydrofluoric acid.

Optically the mineral is uniaxial positive. Birefringence high. Colorless to pale yellow in thin fragments. Pleochroism very weak, colorless to pale yellow. The indices of refraction measured by the immersion method in white light are: $\omega = 1.718$, $\epsilon = 1.819$, $B = 0.101$.

Bastnäsite described as having a prismatic habit, otherwise corresponding closely in its properties to that found in the same district and described in this paper, has been reported by R. S. Dean[5] of the Bureau of Mines.

No chemical analysis has been made on the bastnäsite from New

Mexico, but a qualitative spectrographic examination of a sample of bastnäsite from the Red Cloud area, Gallinas Mountains, Lincoln County, New Mexico, made by K. J. Murata of the U. S. Geological Survey showed the following results:

Major constituents:	La, Ce, F
Minor constituent:	Ca
Traces	Si, Mg, Al, Fe, Ba

Flourine was detected spectrographically (by means of the CaF^+ band) and chemically (by means of the zirconium-alizarin color test). In making the latter test, the mineral was treated with warm HCl which produced an appreciable effervescence ascribable to carbon dioxide liberated from the mineral.

The specific gravity was determined on the Berman balance by M. Fleischer of the U. S. Geological Survey, on fragments from the same sample on which the spectrogram was made. Nine transparent crystal fragments were carefully selected, and each of three determinations was made on three nearly equidimensional fragments. The results are:

Wt. fragments	*Sp. Gr.*
10.8 mg.	4.989
15.2	4.995
16.8	4.991
Average	4.99

X-ray powder diffraction patterns of bastnäsite from the Gallinas Mountains, New Mexico, and of bastnäsite from West Cheyenne Cañon, near Pike's Peak, Colorado (U.S.N.M. No. 84413); and from Madagascar (U.S.N.M. No. R-2617), were made by J. M. Axelrod in the Geological Survey Laboratories. A comparison of these photographs shows that the pattern is the same for all, and that all of the comparable data coincide with those obtained by Oftedal[16] who has made a detailed study of the crystal structure of bastnäsite.

Minerals Associated with Bastnäsite in the Gallinas Mountains

Barite. Barite is one of the most abundant minerals in the bastnäsite-bearing rocks. As much as thirty-seven per cent of the rock mass in some areas is composed of coarse, rough, orthorhombic crystals of barite. Most of the barite is white, but some of it is stained pink from iron oxide; and some is colorless, transparent and glassy. The crystals are short and thick, varying in length from 0.5 millimeter to 6 millimeters. Nearly all

of the crystals are etched and dotted with tiny knobs of purple fluorite. Many of the barite crystals, however, have been dissolved away leaving a honeycomb-like skeleton. In the more altered portions of the rocks the barite has disintegrated to a fine, dust-like powder, and where stained by limonite looks like brown clay. In some areas granular barite has been consolidated into what may be called a barite sandstone.

Barytocelestite (celestobarite). A strontium-bearing mineral that has the same physical properties as the barite described above is found in the southern part of the mineralized region. The mineral is optically biaxial positive, $2V = 45°$; indices of refraction are: $\alpha = 1.628$, $\beta = 1.630$, $\gamma = 1.639$. The optical properties are nearly midway between those for barite and for celestite. Because chemical data are lacking, and the relationship of the indices of refraction to the intermediate compounds not known, the mineral names which were first applied to barium-strontium sulphates have been retained; by the newer system of nomenclature a barium sulphate containing strontium would have the mineral name strontian barite, likewise, barian celestite.

Calcite. Druses of colorless, glassy calcite are found in cavities in the bastnäsite-bearing rocks, and in places calcite occurs as a constituent of the rock mass. The amount of calcite observed is small.

Fluorite. Fluorite with which the bastnäsite is commonly associated occurs in granular masses composed of aggregates of small, deep violet colored crystals loosely held together, usually by interlocking crystals of barite, quartz, and goethite and hematite pseudomorphs after pyrite. As seen in thin section the color varies in different parts of the same crystal, showing bands of different shades of purple lying parallel to the cube faces. In this respect the fluorite resembles that associated with bastnäsite at Jamestown, Colorado.[7] When heated the fluorite shows thermoluminescence, giving off pale yellow, nearly white light, whereas the thermoluminescence of most fluorites is either green or violet. No fluorescence has been observed. The specific gravity is apparently higher (near 3.3) than that for normal fluorite, probably due to inclusions. The index of refraction is also slightly higher (1.440), but this fluorite developed from solutions containing varying amounts of rare earths and other rare elements, and so slight variations in optical properties are to be expected. Bray[3] found by spectrographic study 20 minor elements in the fluorites from Jamestown, Colorado. No spectrographic study was made of the fluorite from the Gallinas Mountains because so much of the fluorite contains impurities.

Goethite. *X*-ray study and microscopic examination indicate that the pseudomorphs after pyrite so common in the bastnäsite rock are goethite with some hematite. In several samples one-fourth, and in a few, one-

half of the rock mass is composed of goethite and hematite pseudomorphs. Well preserved pyrite crystal forms, including pyritohedrons and striated cubes 1 millimeter to 3 millimeters on the edge are common.

Hematite. Hematite is less common than goethite and occurs with goethite in the same crystal in some samples. In others, the pseudomorphs are hematite covered with a thin limonitic film.

Limonitic material. A limonitic material occurs in all of the bastnäsite rocks, and constitutes a large part of the more decomposed rocks. Thin films of iridescent limonite with a metallic luster can be seen also enclosing some of the pseudomorphs.

Orthoclase. A few small grains of orthoclase were found in one sample. The source of the orthoclase is obscure, but it is probable that these grains are relics from the brecciated wall rock.

Pyrite. Pyrite that formed a major constituent of some of the rock during one stage of its history has been acted upon by later oxidizing agents, and what once were pyrite crystals are now goethite and hematite pseudomorphs, some of which are marked by a thin limonitic film with yellow, metallic luster.

Quartz. Small quartz crystals occur commonly scattered in random orientation in the bastnäsite rock. These crystals represent the low-temperature form and show strongly developed prism faces and double terminations. The length of the crystals varies from less than 1 millimeter to 3 millimeters and their length is usually six or eight times their thickness. Most of the crystals are deeply etched, and some are dotted with fluorite crystals.

BASTNÄSITE FROM RUANDA-URUNDI, BELGIAN CONGO (*U.S.N.M. No. 104097*).

Specimens of bastnäsite from the Belgian Congo in the collections of the United States National Museum have not heretofore been studied and so are here described. They consist of six or more irregular, nodular, waterworn fragments one-half to one inch across, of a dense reddish brown, silicified rock, in which bastnäsite occurs as tabular masses, probably rude crystals, 5 to 8 millimeters long and about 2 milimeters wide, scattered at random through the rock. About one-fourth of the rock mass is bastnäsite; other minerals sparsely distributed through the rock are: transparent quartz grains, pyrite crystals, microcline, biotite, and limonite. The entire rock appears to be secondary, but the original source and the occurrence of this rock are unknown.

Some of the tabular masses of bastnäsite were removed and examined. Basal cleavage is conspicuous. The mineral is honey-yellow; some of the grains are reddish brown from staining by iron oxide. Luster resinous.

Hardness 4 to 4.5. Sp. Gr. near 5 (not accurately determined). Infusible. Dissolves in strong sulphuric acid with evolution of hydrofluoric acid and carbon dioxide.

Optically the mineral is uniaxial, positive. Pleochroism weak, colorless to pale yellow. Indices of refraction are: $\omega = 1.722$, $\epsilon = 1.823$, $B = 0.101$. The optical data agree nearly exactly with those for bastnäsite from Bastnäs, Sweden. Physical and optical data on the mineral from Belgian Congo are in such close agreement with known data for bastnäsite that no further study was necessary for conclusive identification.

OPTICAL PROPERTIES OF BASTNÄSITE

For the purpose of comparing the optical properties of bastnäsite from the Gallinas Mountains, New Mexico, and from the Belgian Congo, with those for bastnäsite from previously described localities, three specimens, one from each of the localities most extensively studied and for which the most complete and reliable data are recorded, Sweden, Colorado (Pike's Peak), and Madagascar, were obtained from the United States National Museum for optical study. A brief description of each specimen together with its optical properties is given below.

Bastnäs, Sweden (*U.S.N.M. No. R-2619*). The specimen from Bastnäs is a small fragment of dark gray, granular rock containing honey-yellow grains of bastnäsite in an intimate mixture of cerite, allanite, fluorite, etc. The bastnäsite grains were separated and studied in grain mounts by the immersion method in white light. The mineral is uniaxial positive. The indices of refraction are: $\omega = 1.7220$, $\epsilon = 1.8235$. These data are nearly identical with those determined by Geijer[6] (No. 1, Table 1). The optical properties for the material from Belgian Congo and from Bastnäs are essentially the same. The indices for the bastnäsite from the Gallinas Mountains, however, are slightly lower, indicating a small difference in composition (Table 1).

Pike's Peak, Colorado (*U.S.N.M. No. 84413*). The sample from Colorado is a crystalline mass nearly as large as a man's fist. About half of the mass is reddish-brown, laminated bastnäsite, and the rest of the sample is grayish-buff fluocerite (tysonite). The fluocerite (optically uniaxial negative, $\epsilon = 1.608$, $\omega = 1.613$) appears to occur in parallel growth with the bastnäsite. The optical properties of the bastnäsite are identical with those previously recorded by Larsen (Table 1): Biaxial positive. $\omega = 1.717$, $\epsilon = 1.818$. The optical data for bastnäsite from New Mexico agree closely with those for bastnäsite from Colorado, but those for the material from Belgian Congo are slightly higher (Table 1).

Madagascar (*U.S.N.M. No. R-2617*). The bastnäsite specimen from Madagascar is a piece of a crystal about one inch across and half an inch

thick, and may possibly be some of the pegmatite material described by Lacroix,[12] however, the National Museum has no record of the specific locality or occurrence of the specimen. The color is reddish to yellowish-brown, and with the exception of the typical laminated structure so well developed on this specimen, it might easily be mistaken for monazite, as can be said of most bastnäsite. The mineral is optically uniaxial positive, $\omega = 1.717$, $\epsilon = 1.818$. These properties agree closely with those for bastnäsite from New Mexico (Table 1).

Table 1. Comparison of Optical Properties of Bastnäsite

Locality	Sweden (Bastnäs)		Colorado Pike's Peak		Colorado Jamestown	Madagascar		New Mexico (Gallinas Mtns.)	Belgian Congo
Observer	Geijer[6]	Glass	Larsen[14]	Glass	Glass[7]	Lacroix[12]	Glass	Glass	Glass
Number	1	2	3	4	5	6	7	8	9
$\omega =$	1.7225*	1.7220†	1.717	1.717†	1.716	1.714	1.717†	1.718†	1.722†
$\epsilon =$	1.8242	1.8235	1.818	1.818	1.817		1.818	1.819	1.823
B =	.1017	.1015	.101	.101	.101		.101	.101	.101
Sign	+	+	+	+	+	+	+	+	+

* Indices were determined on prisms cut parallel to the prismatic cleavage.
† Data obtained from recent investigation by the writer.

The optical determinations made on these three specimens, with those determined on bastnäsite from the Gallinas Mountains, New Mexico, and from Belgian Congo, are given in Table 1, together with the data taken from the literature which are included for comparison. Optical determinations by other investigators on material from the previously studied localities, Sweden, Colorado, and Madagascar, are recorded in Table 1, Nos. 1, 3, and 6. Data obtained in the present investigation on material from the same three localities, Nos. 2, 4, and 7, are in close agreement with the recorded data. The uniformity of the optical data for bastnäsite from six localities including the two new ones, New Mexico and Belgian Congo, indicates a nearly constant composition for the mineral, a conclusion arrived at independently from a consideration of the chemical analyses (Table 2).

CHEMICAL COMPOSITION OF BASTNÄSITE

A new cerium-bearing mineral found at Bastnäs, Sweden, and later

TABLE 2. COMPILATION OF CHEMICAL ANALYSES OF BASTNÄSITE

	1	2	3		4		5	6	7	
Ce_2O_3		28.49	29.94		41.04		37.71	40.50		
$(La, Di)_2O_3$ or La group	73.59	45.77	45.77	75.71	34.76	75.80	36.29	36.30	75.84	
CO_2	19.11	19.50	19.50		20.15		20.03	20.20		
F	5.76	5.23	7.42		n.d.		7.83	6.23		
Fe_2O_3							.22			
Na_2O							.18			
H_2O		1.01					.08			
SiO_2	1.25									
P_2O_5								0.60		
Total	99.71	100.00	102.63				102.34	103.83		
$-O=F$			3.11				3.30	2.61		
			99.52				99.04	100.22		
Sp. Gr.			4.93		5.18–5.20 (5.19)		5.12	4.948		

1. "Basiskt" (basic) Fluor-Cerium from Bastnäs, Riddarhyttan District, Sweden. Hisinger's old analysis (1838) recalculated by Nordenskiöld, allowing for CO_2 which Hisinger overlooked (1868).
2. "Hamartite" (Bastnäsite) from Bastnäs, Riddarhyttan District, Sweden. Analysis by Nordenskiöld (1868).
3. Bastnäsite from Bastnäs, Riddarhyttan District, Sweden. Nordenskiöld's analysis with values for Ce_2O_3 and F recalculated by Geijer (1921).
4. Bastnäsite from Cheyenne Mountain, near Pike's Peak, Colorado. Analysis by Allen and Comstock (1880).
5. Bastnäsite from Cheyenne Mountain, near Pike's Peak, Colorado. Analysis by Hillebrand (1899).
6. Bastnaesite from east of Ambositra, Madagascar. Analysis by Pisani, quoted by Lacroix (1912).
7. Bastnäsite from Kychtym (Oural), Ural Mountains, Russia. Analysis by Silberminz (1929).

known as bastnäsite was first analyzed by W. Hisinger,[9] in 1838, and designated by him as "Basiskt Fluor-Cerium från Bastnäs."

Hisinger's analysis taken from the original publication of his work is quoted here:

	funnet (determined)	räknadt (calculated)
Cerfluorid (cerium fluoride)	50.150	49.35
Ceroxid (cerium oxide)	36.430	38.65
Vatten (water)	13.413	12.00
Kiselsyra (silica)	0.007	—

Hisinger concluded that the loss on heating consisted of water and some fluorine but he did not take into account the carbon dioxide. A. E. Nordenskiöld[15] later analyzed the mineral and determined its correct composition. He recalculated Hisinger's analysis considering the carbon dioxide and applying necessary corrections for the reduction of cerium oxide to cerium trioxide and found that the results showed close agreement with his own determinations. To this mineral Nordenskiöld gave the name hamartite. Huot,[10] however had previously called the mineral bastnäsite after the locality. Hisinger's corrected analysis (No. 1), and Nordenskiöld's own analysis (No. 2) are given in Table 2. The chemical composition and physical properties of Basiskt Fluss-spatssyradt from Finbo, described by Berzelius,[2] were recognized by Hisinger as being in agreement with those recorded by him for Basiskt Fluo-Cerium from Bastnäs. Berzelius' analysis, made on scanty material, is incomplete and is not included in Table 2.

A compilation of seven recorded analyses of bastnäsite on material from four widely separated localities is shown in Table 2.

The agreement between the results of the different analysts is remarkable, considering the probable changes in analytical methods in the nearly one hundred years between 1838 and 1929, applied to material containing rare earths. The variations in the percentages are notably small. The combined percentages for the cerium groups, where the greatest difference might occur, vary from 73.59% to 76.80%, with a difference of 3.21%; CO_2 from 19.11% to 20.20%, with a difference of 1.09%; and F from 5.23% to 7.83%, with a difference of 2.60%. If, however, only the more recent analyses had been considered the agreement would be even closer.

OCCURRENCES OF BASTNÄSITE AND ITS ASSOCIATED MINERALS

At the original locality for bastnäsite, Bastnäs, in the Riddarhyattan district, province of Västmanland in central Sweden, bastnäsite and other cerium minerals form narrow bands in a silicate zone, "skarn," composed largely of amphiboles, that run parallel and adjacent to the hematite ore belt, in the leptite (granulite) formation, consisting of leptite, mica schists and limestone-dolomite layers. These narrow bands are fine-grained aggregates of bastnäsite, orthite (allanite), cerite, fluocerite, törnebohmite and other minerals, in a contact metamorphic zone.

At Pike's Peak, Colorado, bastnäsite has been found in parallel growth with fluocerite (tysonite) in feldspar in granite pegmatite.

In Madagascar, east of Ambositra in the region of Torendrika-Ifasina, bastnäsite occurs in a contact metamorphic zone with the pegmatite facies of alkali-granites. The bastnäsite is most closely associated with

tscheffkinite (Chevkinite). Other minerals present are "torendrikite" (glaucophane), aegirite, biotite, hematite, magnetite, rutile, etc. Lacroix[12] describes bastnäsite as occurring also in pegmatite in Madagascar.

In Russia, in the Kyshtymsk (Kychtym) district, in the Urals, bastnäsite is found with cerite, "lessingite" (britholite), törnebohmite, and more abundant orthite (allanite), in pebbles in auriferous gravels. The source of these pebbles has been traced to the contact zone of alkali-syenites.

At Jamestown, Colorado, bastnäsite occurs with cerite and other cerium-bearing minerals (Table 3) in narrow zones and pod-like areas along the contact between pegmatite-aplite bodies in granite and lens-shaped inclusions of biotite schist in the granite.

Bastnäsite in the Gallinas Mountains, as has already been stated, occurs in a brecciated zone near the contact between metamorphosed sediments and igneous intrusives. The mineral assemblage of the deposit (Table 3) and the occurrence are simlar to those at Bastnäs.

The occurrence of the bastnäsite from Belgian Congo is not known.

A tabulated list of minerals associated with bastnäsite together with its occurrences are given for seven recorded localities in Table 3.

Data on mineral relations is meager for some occurrences of bastnäsite. A summary of the available data, however, indicates that the most frequent and most abundant deposits of this mineral are in contact metamorphic zones where these deposits are the result of hydrothermal replacement of sedimentary rocks by mineralizers rich in rare earths and carbon dioxide and fluorine which were derived from nearby igneous intrusions. The largest and only deposit of cerium minerals that has ever produced commercial ore is the well-known contact metamorphic deposit at Bastnäs, Sweden, where during the period 1875 to 1888, a total of 4465 metric tons of high grade cerium ore were mined.[6]

References

1. Allen, O. D., and Comstock, W. J., Bastnäsite and tysonite from Colorado: *Am. Jour. Sci.*, **19**, 390–393 (1880).
2. Berzelius, J., Basiskt Fluss-spatssyradt Cerium från Finbo: *Afhandlingar Fysik, Kemi och Mineralogi (Stockholm)*, **5**,* 64–67 (1818).
3. Bray, J. M., Minor chemical elements in fluorites from Jamestown, Colorado: *Am. Mineral.*, **27**, 769–775 (1942).
4. Dana, E. S., Mineralogical Notes, (3) Tysonite: *Am. Jour. Sci.*, **27**, 481 (1884).
5. Dean, R. S., Bastnaesite at Corona, New Mexico: Notes and News, *Am. Mineral.*, **29**, 3 and 4, 157 (1944).
6. Geijer, Per, The cerium minerals of Bastnäs at Riddarhyttan: *Sveriges Geoloiska Undersökning, Årsbok* **14** (1920), (Stockholm), No. 6, 1–24 (1921).

TABLE 3. OCCURRENCES OF BASTNÄSITE AND ITS ASSOCIATED MINERALS

Local.	Sweden	Colorado		Madagascar	Russia	New Mexico	Belgian Congo
		Pike's Peak	Jamestown				
Occur.	Contact zone	Pegmatite	Contact	Contact	Contact	Brecciated fault	?
	Actinolite	—	—	—	—	—	—
	—	—	—	Aegirine	—	—	—
	Allanite (orthite)	—	Allanite	—	Allanite	—	—
	—	—	—	—	—	Barite	—
	—	—	—	—	—	Barytocelestite	—
	Bastnäsite	*Bastnäsite*	*Bastnäsite*	*Bastnäsite*	*Bastnäsite*	*Bastnäsite*	*Bastnäsite*
	—	—	—	Biotite	—	—	Biotite
	Bismuthinite	—	—	—	—	—	—
	—	—	—	—	—	Calcite	—
	Cerite	—	Cerite	—	Cerite	—	—
	Chalcopyrite	—	Chalcopyrite	—	—	—	—
	—	—	Epidote (brown)	—	—	—	—
	Fluocerite (Tysonite)	Fluocerite (Tysonite)	—	—	—	—	—
	—	—	Fluorite	—	—	Fluorite	—
	—	—	—	—	—	Goethite	—
	—	—	—	Hematite	—	Hematite	—
	—	—	—	Ilmenite	—	—	—
	Lanthanite	—	—	—	—	—	—
	—	—	—	—	Lessingite	—	—
	—	—	—	—	—	Limonite pseudomorphs	Limonite
	Linnaeite	—	—	—	—	—	—
	Magnetite	—	—	Magnetite	—	—	—
	Molybdenite	—	—	—	—	—	—
	—	—	Monazite	—	—	—	—
	—	—	—	—	—	Orthoclase	Microcline
	—	—	Pyrite	—	—	Pyrite	Pyrite
	—	—	Quartz	—	—	Quartz	Quartz
	—	—	—	Rutile	—	—	—
	Törnebohmite	—	Törnebohmite	—	Törnebohmite	—	—
	—	—	—	Tscheffkinite (Chevkinite)	—	—	—
	—	—	Uraninite	—	—	—	—

7. Goddard, E. N., and Glass, J. J., Deposits of radioactive cerite near Jamestown, Colorado: *Am. Mineral.*, **25**, 381–404 (1940).
8. Hillebrand, W. F., Mineralogical Notes, Analyses of tysonite and bastnäsite: *Am. Jour. Sci.*, **7**, 51 (1899).
9. Hisinger, W., Analyser af några Svenska Mineralier, (2) Basiskt Fluo-Cerium från Bastnäs: *Kongl. (Svenska) Vetensk. Acad. Handl.* (Stockholm), 186–193 (**1838**).
10. Huot, J. J. N., Nouveau manuel complet de minéralogie ou tableau de toutes les substances minerales, (*Paris*), **I.**, 296 (269), (1841).
11. Koechlin, R. Bastnäsite von Madagascar: *Centralblatt Mineralogie*, No. 12, 353–354 (**1912**). *Mineralog. und Petrog. Mitteilungen* (Tschermak) **31**, 525 (1912).
12. Lacroix, M. A., Sur l'existence de la bastnaesite dans les pegmatites de Madagascar. Les proprietes de ce mineral: *Bull Soc franç. de Min.*, **35**, 108 (1912).
13. ——— La bastnaesite e la tscheffkinite de Madagascar: *Bull Soc. franç. de Min.*, **38**, 106 (1915).
14. Larsen, E. S., The Microscopic Determination of Nonopaque Minerals: *U.S.G.S. Bull.* **679**, 44 (1921).
15. Nordenskiöld, A. E., Om hydrofluoceritens rätta sammansättnings: *Öfver. Kongl. (Svenska) Vetensk. Akad. Förh.* (Stockholm), **25**, 399–402 (1868).
16. Oftedal, Ivar (Oslo), Über die Krystallstruktur von Bastnäsit: *Zeits. Krist.*, **72**, 239–248 (1929).
17. ——— Zur Krystallstruktur von Bastnäsit, (Ce, La —)FCO_3: *Zeits. Krist.*, **78**, 462–469 (1931).
18. Silberminz, V., Sur le gisement de cerite, de bastnäsite et d'un mineral nouveau, la lessingite, dans le district minier de Kychtym (Oural): Abs. in *Mineral Abs.*, **4**, 150–151 (1929).

Note: * *Dana's System of Mineralogy*, Sixth Edition, page 291, Section 285. BASTNÄSITE: . . . *Afh.* **6**, 64, 1818, should read: *Afh.* **5**, 64, 1818.

QUANTITATIVE SPECTROCHEMICAL EXAMINATION OF THE MINOR CONSTITUENTS IN POLLUCITE

L. H. Ahrens,

Government Metallurgical Laboratory, Witwatersrand University, Johannesburg, South Africa.

Contents

Abstract

Details are given of a quantitative spectrochemical analysis for Tl, Rb, Li, Ga, and K, in two samples of pollucite, one from Karibib, South West Africa, and the other from near Norway, Maine, U.S.A., and the presence of these elements (excluding potassium) within the pollucite lattice is discussed.

The ratio, Rb/Tl, is approximately 50 (Karibib) and 180 (Maine). Both ratios are within the limits of 40 and 440 found in 42 analyses of various Rb- and Tl-containing minerals, chiefly South African, data on which will be published later. Although the former ratio (50) is considerably lower than the mean ratio of the 42 analyses (150) it is worth noting that the mean Rb/Tl ratio for two samples of lepidolite from the same locality was found to be almost identical (70), providing further evidence that Rb and Tl enter different crystal lattices with equal facility.

The presence of a trace of strontium is discussed, and a radioactive origin, involving the transition $Rb^{87} \rightarrow Sr^{87}$, is suggested.

Introduction

Recently, a sample of pollucite from Karibib, South West Africa, was examined at the Union Geological Survey, South Africa, by Nel.[1] This investigation included a qualitative spectrochemical analysis by Dr. B. Wasserstein, who detected, apart from certain other elements, Tl, Rb, Li, and Ga.

The author has been engaged on research on the geochemistry of thallium, gallium, and the three rare alkali metals, and included in this research was the development of a quantitative spectrochemical technique for their estimation in rocks and minerals. In view of the paucity of analytical data concerning these elements in rocks and minerals, and

since, to the knowledge of the author, no analyses exist for thallium, rubidium, and gallium, in pollucite, it was decided to employ the spectrochemical method for a quantitative examination.

Another sample of pollucite from Maine, U.S.A., was kindly placed at the author's disposal by Professor T. W. Gevers of the Geology Department, Witwatersrand University. Unfortunately, only a very small uncleaned piece was available for analysis, so that this sample cannot be regarded as truly representative. However, for one important object of this investigation, that is the determination of the ratio Rb/Tl, the extreme purity of the sample is not of much significance.

In the chemical analysis of the pollucite cited by Nel[1] the potassium and rubidium contents are reported together as mixed oxides; hence it was decided to analyse quantitatively for potassium as well.

Experimental

Details of the spectrochemical technique for the analysis of the above elements in rocks and minerals, together with the underlying principles, will appear in the press at a later date; suffice it to say that the method depends primarily on the volatility of the alkali metals in the arc, using anode excitation and a low amperage. As a result of the ease with which the alkali metals volatilise in the arc, the first fraction of vapours volatilising when rocks, etc., are analysed, consists predominantly of sodium and potassium. Certain other elements, including thallium and gallium (to a lesser extent) also volatilise very readily. The method consists essentially of exposing only the alkali metal rich fraction, on the assumption that under these conditions the effects of extraneous elements are annulled, whence the method may be applied to various rocks and mineral types.

With the assistance of standards containing fifteen per cent of a 1:1 mixture of potassium and sodium carbonates, and using microphotometric measurements, the unknowns are determined.

When pollucite is analysed, the predominant vapour in the arc during the early stages of arcing is caesium, followed by silicon and then aluminium. An argument that might thus be levelled against the method is that in the case of the synthetic standards, a sodium-potassium vapour is predominant in the arc gas column, while in the case of pollucite, the vapour is predominantly that of caesium. Since one important factor influencing the intensities of lines is the composition of the arc gas column, a comparison of line intensities produced on the one hand in a potassium-sodium vapour, and on the other, in a caesium vapour, would at first sight appear to incur difficulty. However, since the alkali metals possess low ionisation potentials, when in quantity they all produce a cooling

effect, and furthermore, since the values of these ionisation potentials are similar, it is reasonable to assume that unless extreme accuracy is desired, the line intensities may be readily compared, irrespective of whether the predominant vapour is caesium or potassium+sodium.

Needless to say, the prepared synthetic standards which contained varying amounts of thallium, rubidium, lithium, and gallium, could not be utilised for the estimation of potassium, for whose determination certain carefully analysed rocks were used as standards.

Results

Table 1 provides the mean values of the analyses, carried out in triplicate.

Table 1. Quantitative Analyses of Pollucite

	% Tl_2O	% Rb_2O	% Li_2O	% Ga_2O_3	% K_2O
Karibib	0.011	0.54	0.021	0.0012	0.49
Maine	0.0013	0.23	—	0.0012	0.76

The lithium content of the sample from Maine could not be determined as a result of the extreme density of the lithium line. Since this sample had not been cleaned and since lithium minerals are commonly associated with pollucite, an analysis would have been of no value.

In the case of the Karibib sample, chemical analysis returned a figure of 1.3% Rb_2O+K_2O, all calculated as Rb_2O. If the above K_2O content is calculated as Rb_2O and added to the Rb_2O found, a total of 1.5% is obtained, which is in reasonably good agreement with the chemical result of 1.3%.

Discussion

Before providing a brief discussion on the occurrence of Tl, Rb, Ga, and Li, in pollucite, a short account will be given of certain salient factors underlying the formation of this caesium mineral, in contrast with the fact that no discrete mineral is formed by the commoner rare alkali metal, rubidium.

Residual phases of differentiation are commonly relatively rich in ions of large dimensions, in accordance with the fact that when two (or more) ions of slightly different sizes, but of like valency, compete for a similar site within a given growing lattice, the smaller ion is generally more acceptable, the larger ion being relatively enriched in the mother liquor fraction. Thus we find Cs^+, Rb^+, and Tl^+, all ions of large dimensions, continually rejected during differentiation and enriched in the residua of differentiates. The degree of enrichment will depend to a large extent

on the relative radii of the ions in question, the larger the ion the greater the degree of enrichment.

The radius of Cs^+ is greater than that of Rb^+ and Tl^+ (its radius is greater than that of any other ion), with the result that when caesium, rubidium, and thallium substitute for potassium, which they invariably do, in potassium rich minerals ($K^+ = 1.33$, $Rb = Tl = 1.49$ and $Cs^+ = 1.65$Å), since Cs^+ is the largest ion, it is acknowledged with relatively greater reluctance than Rb^+ and Tl^+. The result is that caesium tends to concentrate relatively to rubidium and thallium in the residual differentiates. Thus, although rubidium is considerably more abundant than caesium in the earth's crust (Atomic ratio Rb/Cs = approx. 50), no rubidium mineral has ever been reported resulting from differentiation, whereas, as a result of the relatively greater enrichment of the larger caesium ion, this less abundant element does on occasion form the caesium mineral, pollucite.

(*1*) *Rubidium and Thallium*

Since rubidium and thallium behave in approximately the same manner as caesium during differentiation, the presence of relatively appreciable quantities of these two elements in pollucite is to be expected. Furthermore, since the radii of Rb^+, Tl^+, and Cs^+, are of the same order, Rb^+ and Tl^+ undoubtedly occur in substitutional solid solution replacing Cs^+.

From Table 1, the ratio Rb/Tl is 50 (Karibib) and 180 (Maine). The former ratio is somewhat less than the average ratio of about 150 found in 42 analyses of various minerals, although it lies within the extreme limits of 40 and 440 found in these analyses. Analyses of two lepidolites from the same locality (Karibib) also revealed low Rb/Tl ratios. Table 2 provides the mean results of the analyses of these two samples.

Table 2. Quantitative Analysis of Lepidolite

% Tl_2O	% Rb_2O
0.021	1.60

In this case the ratio Rb/Tl is 70, which to all intents and purposes can be regarded as being equal to the ratio for pollucite, when taking into account slight regional variations and experimental errors.

Apart from the fact that the ratios in both samples of pollucite fall within the limits of 40 and 440, this constancy of the ratio Rb/Tl in two entirely different minerals from the same locality, provides an interesting confirmation of what has been concluded from the results of the 42 analyses mentioned above, and that is: excluding those phases where

thallium enters sulfide minerals, rubidium and thallium comprise a pair of elements, remarkable in the constancy of their relative proportions, this constant relationship apparently being independent of the mineral type and holding over all ranges of concentration. The essential underlying factors determining this constant relationship is that both Rb^+ and Tl^+ are monovalent ions, the radii of which are identical.

(*2*) *Gallium*

The presence of gallium in almost all aluminium-rich minerals is now well established as a result, chiefly, of the work of Goldschmidt and Peters,[2] Al^{+++} (radius = 0.57Å) being replaced by Ga^{+++} (radius = 0.62Å). The ratio Al/Ga is, however, by no means constant and varies very considerably even when only taking into account Al silicate minerals of igneous origin. It is a little surprising to find only 0.0012% Ga_2O_3 in both samples of pollucite, since gallium tends to concentrate relatively to aluminium as a rule, in residual phases. The gallium content of the lepidolite from Karibib is twenty times as much as that of the pollucite (0.025% Ga_2O_3). A relatively high gallium content appears to be characteristic of lepidolites and also muscovites.

It is not quite clear why pollucite is poor in gallium, although Goldschmidt has pointed out that the chemical characteristics, chiefly the pH, of the solutions play a very important part in influencing the Al/Ga ratio, which is apparently in delicate balance.

(*3*) *Lithium*

Although Li is a relatively small ion (radius 0.78Å) it is also rejected during differentiation and tends to concentrate in late pegmatitic phases, together with the other rare alkali metals and thallium. However, the reasons for this rejection are different from those outlined for the late enrichment of the large ions. Although Li^+ is capable of replacing Mg^{++} and Fe^{++} in the ferromagnesian lattices ($Mg^{++} = 0.78$, $Fe^{++} = 0.83$Å) it is not readily accepted, probably as a result of the monovalency of the lithium ion and its resultant weak attraction, relative to the divalent ions. Lithium cannot be accommodated, either in the plagioclase or potash feldspars, or in quartz, since none of these mineral structures contain ions in sixfold co-ordination. Micas do contain small amounts of lithium, which is only to be expected, since one essential feature of the structure of the mica lattice is that it includes sites for ions capable of sixfold co-ordination. However, probably as a result of the monovalency of lithium, ions of higher potential enter the earlier micas preferentially. For these reasons, lithium is present in quantity in only very late dif-

ferentiates (Li micas and other lithium minerals). As is to be expected, pollucite is commonly associated with lithium minerals.

As a result of this association it is not surprising to find a small quantity of lithium in pollucite. However, whether the lithium is present in small amounts of lithium minerals as impurities, or not, cannot be definitely established. The Karibib sample had been carefully cleaned and we may therefore assume that at least part of the lithium occurs within the pollucite lattice itself. It is extremely unlikely that lithium is capable of replacing Cs, although Nel has suggested a mechanism whereby Cs^+ is replaced by $Na^+ + H_2O$. In a like manner $Li^+ + H_2O$ might be capable of replacing Cs^+. It should also be borne in mind that pollucite possesses a lattice, the structure of which is fairly open and which, unlike the more closely packed types, is possibly conducive to considerable interstitial movement of ions, particularly small ones like Li^+. It is therefore quite likely that part of the lithium is held within the pollucite lattice in interstitial solid solution.

Radioactive Disintegration of Rubidium

Both potassium and rubidium are naturally radioactive, their radioactivity being characterised by the emission only, of beta particles. By losing a beta particle, the rubidium isotope of mass number 87 is transformed into a strontium isotope of equivalent mass number. (It is believed that only Rb^{87} is radioactive.) It is thus possible that the strontium contained in certain minerals is essentially that of mass number 87, that is, derived from the radioactivity of rubidium. For example, Mattauch[3] has been able to establish, by means of mass spectra, that the strontium present in a rubidium-rich mica from Canada is predominantly that of mass number 87, ordinary strontium being present in only negligible traces.

If we assume the half life period of rubidium to be 2.3×10^{11} years, and the age of the later phases of the Old Granite of South Africa, in which the Karibib pollucite occurs, to be approximately 9.0×10^8 years, then the amount of strontium that would have accumulated from 0.54% Rb_2O during this period is 0.0014%.

A careful spectrochemical examination of the Karibib pollucite, necessitating arcing to completion as a result of the very late appearance of the strontium spectrum, revealed definite traces of strontium. Unfortunately a quantitative method for determining the strontium content was not at hand, although an approximation could be made, which indicates that the strontium is present in quantities greater than 0.001%, but less than 0.004%, thus suggesting a radioactive origin. Another factor which

suggests a radioactive origin for the strontium is the absence of barium. Thus, although strontium and barium do not constitute a coherent pair of elements in the same sense as do rubidium and thallium, they are nevertheless invariably associated. Furthermore, since the radius of Ba^{++} is greater than that of Sr^{++} (1.43 and 1.27Å, respectively), there is often a tendency for Ba^{++} to concentrate relative to Sr^{++} in later phases of differentiation. However, as the barium concentration is below the limit of detection (below about 0.0001% Ba), this further suggests that the genesis of the strontium in the Karibib pollucite may be ascribed to the radioactivity of rubidium.

Acknowledgments

I wish to thank Mr. H. J. Nel and Professor T. W. Gevers, for kindly placing at my disposal the two samples of pollucite from Karibib and Maine, respectively. Thanks are also due to Professor L. Taverner, Director of the Government Metallurgical Laboratory, for permission to publish this investigation.

References

(1) Nel, H. J., Pollucite from Karibib, South West Africa: *Am. Mineral.*, **29**, 443–452, 1944.

(2) Goldschmidt, V. M., and Peters, Cl., Zur Geochemie des Galliums: *Nachr. d. Ges. d. Wiss. Göttingen, Math.-Phys. Kl.*, **1**, No. 11, 165–183 (1931).

(3) Mattauch, J., Das Paar Rb^{87}-Sr^{87} und die Isobarenregel: *Naturwiss.*, **25**, 189 (1937).
Mattauch, J., Massenspektrographie und Kernbaufragen: *Naturwiss.*, **25**, 738 (1937)

COLUMBIUM AND CERIUM MINERALS IN MONTANA

S. R. B. Cooke* and Eugene S. Perry**

Abstract

Rare minerals of the fergusonite and allanite groups, containing yttrium, scandium, columbium and cerium, occur in many places of southwestern Montana. They are found in granite pegmatite, in part pre-Cambrian, in part late Cretaceous or early Tertiary age. Some material is radioactive. As yet the occurrences have not been proven to be of commercial importance.

Geologic and Geographic Occurrence

Widely scattered occurrence of rare minerals containing yttrium, scandium, columbium and cerium in southwestern Montana has recently been recognized, and three new varieties have been identified. Some of the material is radioactive. Little or no attention has been paid to these columbium- and cerium-bearing minerals during the long mining history of Montana, mainly because they occur in coarse-grained granite pegmatite dikes not mined for ores, and also possibly because they superficially resemble black tourmaline which is rather plentiful in pegmatites in this region. Although no commercial significance is attached to these discoveries at present, they do open up a large field for investigation, since the mineral content of these pegmatites has not been studied critically.

Hundreds of massive pegmatite dikes are known to be present in this region, which is from one to two hundred miles across. They show as large bold outcrops, called "quartz blowouts" by prospectors, and from the highways they appear as conspicuous white blotches on an otherwise gray somber landscape. These bodies are typically lenticular, commonly 10 to 20 feet in width, and 50 to 300 feet in length. Two or three lens-like outcrops may be linearly arranged along a distance of 1000 yards or more, suggesting a hidden continuity.

Some of the dikes appear to be of pre-Cambrian age, because of their intimate association with a series of Archean or Huronian schists and gneisses, their lack of association with Cambrian strata, and because of the presence of boulders and fragments of pegmatitic material similar to that of the dikes in a late Proterozoic (Belt series) conglomerate which lies unconformably above the metamorphic complex. Other dikes of this type are definitely associated with the late Cretaceous granitic intrusives prevalent in southwestern Montana. Geologic age of the dikes is particularly significant since it is noted that the two observed occur-

* Research Professor of Mineral-Dressing, Montana School of Mines.

** Professor of Geology, Montana School of Mines.

rences of the columbium mineral are in areas of pre-Cambrian rocks, and that those of the cerium minerals are in areas of late granites.

The material examined comes from five widely separated localities near Sappington, Laurin, Boulder, Homestake and Janney; the first two in pre-Cambrian areas, the last three in areas of late granitic rocks. The occurrences are somewhat complicated in that the Laurin, Boulder and Homestake materials were found in placers and not in place, although the presence of nearby pegmatites is suggestive of their ultimate origin. The widespread distribution of these occurrences leads the writers to believe that careful search would lead to numerous localities where these minerals might be found in pegmatite dikes.

The so-called "Sappington Mica Mine," about eight miles south of the small station by that name, is in a typical granite-pegmatite which lies parallel to the gneissic structure in a complex mass of hornblende and biotite gneiss. Perhaps 95 per cent of the pegmatite is feldspar and quartz. Orthoclase is dominant, but some oligoclase may be present. Black tourmaline occurs sparingly. The quartz is generally milky, or snow-white, but transparent and rose quartz is present, and it commonly shows a rudimentary cleavage. The dike is about 25 feet wide at its thickest place. Through the central part of the dike is a zone 5 to 10 feet thick in which "books" of muscovite mica are plentiful, and the columbium-bearing mineral occurs in scattered grains and in lumps up to two inches in diameter in the muscovite zone. The muscovite amounts to less than 1 per cent of the pegmatite.

The material from near Laurin appears to be fairly plentiful and was discovered in gravel of a bench-placer being worked for gold. The placer is about four miles east of Laurin on California gulch not far from its head. The entire area is underlain by the basal complex of schist and gneiss, locally cut by quartzitic pegmatite dikes.

The material from near Boulder also comes from gold placers about ten miles south of the townsite. Only two pieces about one inch in diameter were obtained, but it is reported that more is present. The placer lies on the eastern edge of the Boulder batholith (late Cretaceous quartz monzonite) which is locally cut by numerous aplite dikes and occasional pegmatite bodies.

The material from near Homestake comes from placers in a creek draining into Lake Delmoe which is six miles northeast of the railroad station. There is reported to be about one pound of the mineral per cubic yard of gravel.

The fifth sample comes from a pegmatite body near Janney, a small station on the Milwaukee railroad about ten miles south of Butte. The

pegmatite is essentially quartz with some feldspar, and the cerium-bearing mineral occurs as isolated lumps in the rock mass.

Only where the pegmatite has been opened by pits were the two occurrences in situ of these rare minerals observed. They are not recognizable in the weathered outcrops, which show only quartz and feldspar; apparently they decompose by weathering to a rusty mass of limonite. It is probably this condition which has resulted in their oversight through the long years of prospecting in Montana, because pegmatite dikes in Montana are commonly considered barren of minerals of ready commercial value. If Montana pegmatites were worked on a large scale for their content of orthoclase or muscovite, it is probable that much more of this type of material would come to attention.

Mineral Characteristics

The mineral from near Sappington is massive with a conchoidal fracture, dark brown in color, and resinous. Carefully concentrated material has a specific gravity of 3.95. The hardness is slightly over 5, and it is infusible in the blow-pipe flame. The mineral is radioactive.

The Laurin mineral is massive, jet black, and has a conchoidal fracture. The specific gravity is 5.6, the hardness is 6, and it is infusible in the blowpipe flame. This mineral is also radioactive, but less so than the Sappington mineral.

The material from south of Boulder is massive, jet black, with uneven fracture; specific gravity is 3.9, or slightly over, and hardness is slightly over 5. This mineral fuses easily in the blowpipe flame with intumescence yielding a black slag. The mineral is not radioactive.

The mineral from Homestake and Janney is very similar to that last mentioned, although the hardness and specific gravity are slightly different.

Optical Properties

All five minerals were examined by the immersion method without the benefit of a universal stage. The refractive index of the Laurin mineral was measured in a sulfur-selenium melt. Indices of the other minerals were obtained in media prepared by mixing phosphorus, sulfur and methylene iodide.[1] Indices of these last mentioned mixtures were measured directly with a Fisher refractometer,[2] reading to $n = 1.900$.

[1] West, C. D., Immersion liquids of high refractive index: *Am. Mineral.*, **21**, 245–249 (1936).

[2] Fisher Scientific Company, Pittsburgh, Penna.

The optical properties of all four minerals are tabulated below.

Sappington	*Laurin*	*Boulder*	*Janney*
Lemon-yellow	Dark brown	Light brown	Light brown
Isotropic	Isotropic	Biaxial (−)	Biaxial (−)
$n=1.830$ to 1.840	$n=2.120^{\pm}.005$	$\alpha=1.769$	$\alpha=1.781$
		$\beta=1.795$	$\beta=1.802$
		$\gamma=1.805$	$\gamma=1.810$
		$\gamma-\alpha=0.036$	$\gamma-\alpha=0.029$
		$2V=60°$	$2V=60°$
		Dispersion weak	$r>v$, strong
		X, light brown	X, light straw-brown
		Y, brown	Y, brown
		Z, very dark brown, almost opaque	Z, very dark red-brown

The optical properties of the mineral from near Homestake are practically the same as those of the Janney mineral.

X-ray Analysis

The Sappington material has been studied at Harvard University where Dr. Clifford Frondel has made *x*-ray powder photographs of the ignited mineral. He decided that it showed similarity in pattern and line intensity to material from Petaca, New Mexico, and Ytterby, Sweden; and that all three specimens are fergusonite. Differences in pattern and line intensity are attributed to differences in chemical composition, possibly to different tantalum-columbium ratios which have not been determined for all of the material. It is not definitely known how this ratio affects properties in this mineral.

Chemical Composition

Quantitative chemical analyses of these minerals are at present difficult to obtain because of the rare elements present. Comparative spectrographic analyses show that columbium is the major element in the Sappington and Laurin minerals. The other three minerals are more complex, at least with respect to the major elements.

Spectrographic analyses of the five samples were made on a five foot Wadsworth grating spectrograph. By comparison of individual spectra, and of these with the spectra of standard samples, the following semi-quantitative results were obtained. The nomenclature corresponds approximately to that of Merriam and Kennard.[3]

Elements listed under "Trace" are in the order of their atomic num-

[3] Merriam, R., and Kennard, T. G., An unidentified mineral in the quartz basalt of Lassen Volcanic National Park, California: *Am. Mineral.*, **28**, 602–604 (1943).

bers. The other entries contain the elements in the approximate order of their abundance. Other elements having sensitive arc lines were searched for, but were not found.

Qualitative chemical tests show that considerable amounts of phosphorus are present in the Boulder, Homestake and Janney minerals, but absent from the other two.

	Sappington	*Laurin*	*Boulder*	*Janney and Homestake*
Large amount	Cb	Cb	Ce	Ce
	Y	Sc	Ca	Ca
	Sc	Sm	Al	Al
	Fe	Y	Ti	Ti
			Si	Si
Small amount	Ti	Fe	Fe	Fe
	Ba	Ca	Mn	Mn
	Si	Ti	Nd	Nd
	Ca	Sn		
	Ta	Gd		
	U	Dy		
	Sm			
	Yb			
Very small amount	Al	Ba	Mg	Mg
	Pb	Pb		
	Dy	Mn		
	Nd	U		
	Eu	Nd		
	Gd	Er		
	Er	Yb		
	Th	Lu		
Trace	Mg	Mg	V	V
	V	Al	Sr	Cu
	Cr	Si	Y	Sr
	Mn	V	Cb	Y
	Co	Cu	Ag	Cb
	Cu	Sr	Ba	Ag
	Sr	Ag	Sm	Ba
	Ag	La	Gd	Sm
	Ce	Ce	Dy	Gd
	Ho	Ho	Ho	Dy
	Lu	Ta	Er	Ho
		Th	Yb	Er
			Lu	Yb
			Pb	Lu
				Pb

Conclusions

The rare earth minerals herein described are members of two different isomorphous groups, and are variants within each group not identical with described species. The columbium-bearing mineral belongs to the fergusonite group, and the cerium-bearing mineral belongs to the allanite group.

The specific gravity of the Sappington mineral (3.95) is markedly less than that of commonly described fergusonite (5.38 for fergusonite containing 54.07 Cb_2O_5 and no tantalum.[4] This reference states that specific gravity decreases "markedly with hydration"). The index of refraction (1.84) is also notably less than those given by Larsen[5] (2.115 to 2.19). It is possible that part of this discrepancy is due to the relatively high scandium content as indicated by the spectrographic analyses. Scandium is not reported in the 13 analyses given by Dana (seventh edition), and necessarily must have been very low, because each of the analyses totals to close to 100 per cent, or else this element was included with other elements. The Laurin mineral conforms to the fergusonite group in all determined properties except for its scandium content.

The minerals from near Boulder, Homestake, and Janney are similar in physical properties and almost identical in composition. All are believed to be members of the allanite group.

[4] Palache, C., Berman, H., and Frondel, C.: *Dana's System of Mineralogy*, seventh ed., vol. **1**, p. 760 (1944).

[5] Larsen, E. S., and Berman, H., The Microscopic Determination of the Non-opaque Minerals: *U.S.G.S. Bull.* **848**, Sec. Ed., pp. 62–64 (1934).

LITHIOPHORITE FROM THE POSTMASBURG MANGANESE DEPOSITS

J. E. De Villiers,*
Geological Survey of the Union of South Africa, Pretoria.

With Chemical Analyses by C. F. J. van der Walt

Introduction

In Dana's *System of Mineralogy* lithiophorite is described as a hydrated manganese ore containing 10–15% Al_2O_3, 1.2–1.4% Li_2O and 12.6–15.4% H_2O. In the past it has generally been looked upon as a variety of "psilomelane" but in 1932 Ramsdell (1) found that it gives a distinctive *x*-ray photograph and is thus an independent mineral species. The formula has been given by Fleischer and Richmond (2) as possibly $Li_2(Mn^{II}, Co, Ni)_2Al_8Mn_{10}{}^{IV}O_{35} \cdot 14H_2O$. Up to the present no ore-microscopical or crystallographic data for the mineral have, as far as I know, been published.

Lithiophorite was first recognised in the Postmasburg ores in 1943. It was originally distinguished by means of chemical tests but after its ore-microscopical properties and etch reactions had been determined it could be readily identified by means of these properties. In the past I have found it either as very fine-grained material, or as small flakes, very sparingly disseminated through a sitaparite ore (see Fig. 1). Recently, however, a few specimens of coarsely crystalline lithiophorite were obtained from the farm Gloucester near Postmasburg. These are exceptionally well suited for study and some of the physical, ore-microscopical and chemical properties of the mineral have accordingly been determined. The results obtained are given in this paper.

The specimens are coarse-grained and black; as received they were partly coated with brown ferruginous clay which could be washed off. On fresh surfaces they present a glistening appearance due to the reflection of light from many cleavage planes and in part they are lined with crystals which project into vugs (see Fig. 2). The samples are composed predominantly of lithiophorite, the other minerals present being braunite, sitaparite, psilomelane, and a trace of hematite. It is believed that, in common with the Postmasburg manganese ores generally, they were deposited by solutions which were either wholly, or in part, of magmatic origin. The specimens are described more fully in a subsequent section.

* Since I submitted this manuscript for publication it has come to my notice that Dr. J. W. Gruner identified lithiophorite in the Postmasburg manganese ores a few years ago. See *Am. Mineral.*, **28**, 174 (1943), also **28**, 615 (1943).

FIG. 1. Polished section showing lithiophorite with dark-coloured diaspore and sitaparite (mineral with square outlines). ×170.

FIG. 2. Specimen of coarsely crystalline lithiophorite. Note crystals; and films of braunite encrusted with lithiophorite. About $\frac{2}{3}$ natural size.

Physical Properties of the Lithiophorite

The colour is iron black with a bluish tinge. Streak is greenish black. Specific gravity = 3.37 (±0.02). This value was obtained by immersing small grains of the mineral in Clerici's solution, diluting until neither floating nor sinking occurred and measuring the specific gravity of the liquid. Cleavage in one direction, micaceous. Laminae somewhat flexible and sectile. Hardness = $2\frac{1}{2}$ to 3. This varies with the crystallographic direction and is least on the cleavage face.

The crystal faces are usually curved and slightly corroded. They are thus unsuitable for goniometric measurement. On the cleavage surfaces the outlines of the crystals are hexagonal and rude measurements indicate that the angles approximate 60°. Such surfaces generally show striations, probably due to twinning, which divide the hexagons into six sectors. It is considered likely that the mineral is hexagonal or pseudo-hexagonal.

Ore-microscopical Properties

The colour in polished section varies from light grey to dark brownish grey, the pleochroism being exceptionally strong. In the brightest direction the reflectivity is about equal to that of braunite, i.e. about 18%, while in the darkest direction it is probably less than half of this figure. The anisotropic effects are extreme and the polarisation colours light grey to dark brown and bluish grey. Sections parallel to the cleavage face have the highest reflectivity and show no pleochroism or anisotropism. Lithiophorite is relatively little affected by the etch reagents ordinarily employed to distinguish between the manganese oxides. HCl (conc.) has no effect and the action of $H_2O_2+H_2SO_4$ [equal parts of H_2SO_4(1:1) and H_2O_2 (5%)], $SnCl_2$ (sat. soln. in conc. HCl) and HF (comml. conc.) are negative, or very feeble if the reagent is left on for one minute. On prolonging the time of the reaction, the effect of HF and $H_2O_2+H_2SO_4$ becomes more marked.

Chemistry

A chemical analysis of lithiophorite was carried out by Dr. C. F. J. van der Walt of the Division of Chemical Services. The sample analysed was prepared by selecting small, clean cleavage flakes and is considered to have been of excellent purity.

According to qualitative chemical tests, cobalt and nickel are either absent or present only in traces.

In calculating the formula of lithiophorite, SiO_2 and Fe_2O_3 have been neglected. The amount of the former constituent is very small and, as was concluded in the case of the analysis given in Table 2, the Fe_2O_3 probably represents admixed impurity.

TABLE 1. ANALYSIS OF LITHIOPHORITE FROM GLOUCESTER

	%	Mol. rat.	At. rat.			Alternative At. ratios		
MnO	48.15	0.6787	Mn^{III}	0.231	1.02	Mn^{II}	0.116	1.02
O	9.01	0.5631	Mn^{IV}	0.447	1.97	Mn^{IV}	0.563	4.94
Al_2O_3	23.84	0.2339	Al	0.468	2.06	Al	0.468	4.11
Fe_2O_3	0.96	0.0060	—	—	—	—	—	—
Li_2O	3.30	0.1104	Li	0.221	0.97	Li	0.221	1.94
H_2O+	13.15	0.7298	H_2O	0.730	3.22	H_2O	0.730	6.40
H_2O-	1.45	—	—	—	—	—	—	—
SiO_2	0.30	—	—	—	—	—	—	—
CaO	Tr.	—	—	—	—	—	—	—
Na_2O, K_2O	Nil	—	—	—	—	—	—	—
	100.16							

Analyst: C. F. J. van der Walt.

The analysis presents the difficulty that only the total amount of the available oxygen can be determined. There is no means of determining chemically the amount of manganese of any particular valence present. Two arrangements of the analysis are therefore possible, one in which the manganese is 3- and 4-valent, and the other in which it is 2- and 4-valent, viz:

$$Li\ Mn^{III}\ Mn_2^{IV}\ Al_2O_9 \cdot 3H_2O$$
$$Li_2\ Mn^{II}\ Mn_5^{IV}\ Al_4O_{18} \cdot 6H_2O.$$

Below, the analysis of lithophorite from Bishop, Postmasburg, is given. This was made in 1943 on material described in a subsequent section.

TABLE 2. ANALYSIS OF LITHIOPHORITE FROM BISHOP

	%	Mol. rat.	At. rat.			Alternative At. ratios		
MnO	44.9	0.6330	Mn^{III}	0.253	1.20	Mn^{II}	0.127	1.27
O	8.1	0.5063	Mn^{IV}	0.380	1.81	Mn^{IV}	0.506	5.06
Al_2O_3	22.0	0.2158	Al	0.432	2.06	Al	0.432	4.32
Fe_2O_3	10.5	0.0657	Fe^{III}	0.131	—	—	—	—
Li_2O	2.7	0.0904	Li	0.181	0.86	Li	0.181	1.81
H_2O+	11.7	0.6494	H_2O	0.649	3.09	H_2O	0.649	6.49
SiO_2	0.1							
	100.0							

Analyst: C. F. J. van der Walt.

If the Fe_2O_3 is considered as part of the lithiophorite molecule, the above analysis leads to the formula: $Li_2(Mn''', Fe''')_4Mn_4^{iv}Al_4O_{21} \cdot 7H_2O$, which differs considerably from that of the fairly pure material from Gloucester.

It is thus concluded that the Fe_2O_3 is probably present as an impurity. Disregarding the Fe_2O_3, the analysis gives the formula: $Li\ Mn^{III}Mn_2^{IV}Al_2O_9 \cdot 3H_2O$. This is the formula deduced for the Gloucester material, but the agreement with the analysis is less close.

Description of the Specimens

As stated previously, the specimens are coarsely crystalline, the diameters of the individual grains of lithiophorite varying from a few millimetres to about a centimetre. In part they are rudely botryoidal and show protruding crystals. Braunite, partly altered to psilomelane, is found in the cores of the botryoidal masses and from a macroscopic examination it appears as if the lithiophorite was in large part deposited on the braunite in cavities. In a few of the cavities thin films of braunite (usually encrusted with lithiophorite) may be observed. These apparently originated as veins in some rock which was later dissolved, leaving behind the braunite. Subsequently lithiophorite was deposited on the films (see Fig. 2). Braunite predominates in one specimen and the lithiophorite forms lenticles and irregular patches in the ore.

The grain size of the braunite is much smaller than that of the lithiophorite (0.01–0.1 mm.). In polished section it can be seen that the boundaries between the two minerals are either irregular and fretted or the braunite is idiomorphic towards the lithiophorite. In part these boundaries are obscured by the development of psilomelane as an alteration product. The braunite often occurs as veinlets and if sitaparite is present it again veins the braunite. Hematite occurs very sparingly as small scattered grains chiefly in the sitaparite. The order of crystallisation of the main minerals comprising the specimens appears to be as follows:—

(1) Braunite, (2) sitaparite, (3) lithiophorite.

Part of the braunite however, like the psilomelane, may have been formed through the alteration of earlier minerals and this braunite would therefore be younger than the lithiophorite. Between the periods of deposition of the sitaparite and the lithiophorite there was evidently a period of solution.

The lithiophorite from Bishop, the analysis of which is given in Table 2, has a purplish-black colour and is extremely fine-grained (grain size for the most part is less than a hundredth of a millimetre). It occurs as lay-

ers, a few millimetres thick, in a laminated psilomelane-hematite ore. The sample submitted for analysis was judged to be fairly pure, the only impurity observed in polished section being a very small amount of hematite. The amount of this, however, could not be estimated.

References

1. Ramsdell, L. S., An x-ray study of psilomelane and wad: *Am. Mineral.*, **17**, 143–149 (1932).
2. Fleischer, M., and Richmond, W. E., The manganese oxide minerals: (A Preliminary Report) *Econ. Geol.*, **38**, 269–286 (1943).

THE OCCURRENCE AND HARDNESS OF INDIUM

Roy D. McLellan*

Abstract

Microscopical and spectrographic studies made on a large number of ore deposits from this and other continents, revealed that the indium content of primary ores occurs predominantly in the lead sulfide.

Present data indicate that indium is the softest of all the metals. It is considerably softer than talc. Some of the physical and chemical properties of indium are discussed.

Occurrence

Indium occurs in nature predominantly in association with lead minerals. A survey of sulfide ores from a large number of widely scattered localities showed the indium to occur largely in apparent solution in the lead sulfide. The various ore minerals were crushed to 60–100 mesh and optically pure mineral particles were hand picked under the microscope. Their indium content was determined with the spectrograph.

Pure In_2S_3 is an amber-colored strongly pleochroic substance possessing extremely high indices of refraction, birefringence and dispersion. It should therefore lend itself to detection, even when present in very minute quantities, in indium-bearing galena. The failure to detect this compound in any of the indium-bearing specimens examined indicates an appreciable solid solubility of In_2S_3 in galena.

Moderate concentrations of indium were found in some oxidized zinc minerals such as hemimorphite and smithsonite. In many other instances little concentration of indium was seen in the oxidized zinc minerals.

In the course of treatment at the smelters and refineries the indium tends to concentrate with the zinc and cadmium and this, no doubt, has given rise to the erroneous observation that indium occurs in nature largely in association with zinc minerals. Indium is frequently observed in relatively large quantities in primary zinc sulfide ores but its actual occurrence in them is typically in the galena associated with these zinc and cadmium minerals. Only moderate amounts of indium were observed in any of the hand picked particles of sphalerite.

Powder photographic data from x-ray studies of indium are said to indicate an arrangement of its atoms at the points of a face-centered tetragonal lattice of axial ratio $c:a=1.06$. The lengths of the edges of this unit tetragonal prism are $a=4.58$Å, $c=4.86$Å.[1]

* Petrographer and Spectroscopist, Central Research Laboratory, American Smelting and Refining Company, Perth Amboy, New Jersey.

[1] Hull, A. W., X-ray crystal analysis of thirteen common metals: *Phys. Rev.*, **17**, 571 (1921).

The specific gravity of extruded or hammered indium is 7.32. It melts at 155°C. According to measurements made by the writer, and based on the relative time required to volatilize a given quantity of the pure metal in the carbon arc, the boiling point of indium is 2610°C. The interval between the melting point and the boiling point of indium is larger than that of any other metal in this temperature range.

Indium imparts a deep blue coloration to the gas flame. Its compounds yield a blue flame tinged with colors produced by the various elements involved. In the carbon arc the color of the blue flame from metallic indium or its compounds is considerably lighter in shade than that in the much lower temperature of the gas flame.

In the carbon arc surrounded by air, metallic cadmium, zinc, aluminum and all other more electropositive elements are rapidly converted to oxides. Those portions of the oxides in contact with the hot carbon are gradually reduced to metal which volatilizes together with lesser amounts of oxide vapors.

Metallic indium, however, behaves like tin or lead in the carbon arc and remains as a metallic globule until completely volatilized. Indium oxide is reduced to metallic indium in the open carbon arc.

When heated with the blowpipe flame, indium is oxidized with difficulty. Before the blowpipe on charcoal a yellowish-gray coating is ultimately formed near the assay.

When pure indium is burned in the carbon arc, a coating of In_2O_3 forms on the upper electrode. At higher temperatures (but below a red heat) this coating is brown or tan-colored. On further cooling it changes to brownish yellow and later to bright canary yellow. When cold its color is pale yellow or yellowish white. Indium oxide yields colorless bead tests.

Metallic indium dissolves quietly and rapidly in nitric acid. Only slightly less rapid is the action of hydrochloric acid on indium. This causes considerable boiling and effervescence due to the liberation of hydrogen. Indium dissolves slowly in dilute sulfuric acid.

Indium is a silvery-white metal of the aluminum family. Its color is lighter than that of tin and when freshly rolled it possesses a color tone resembling but considerably lighter than aluminum.

Metallic indium is resistant to chemical corrosion and its surfaces are practically unaffected by air or water. The metal is very malleable and ductile.

Hardness

Metallic indium is softer than any other known metal or alloy. Some of the alkali metals, if equally pure and free from oxidation products,

might possibly be as soft or even softer than indium. When cut with a knife, indium tends to adhere to the blade. Pieces of indium can be welded at room temperature by pressing them together with the fingers.

The scratch hardness of high purity indium was compared with that of pure transparent foliated talc. The purity of this talc was checked by the spectrograph and by index of refraction measurements with the petrographic microscope.

The talc proved to be considerably harder than the indium. Slender bundles of talc folia readily scratched the indium. The surfaces of the talc folia could not be scratched by the indium. The hardness of indium is therefore less than unity on Mohs' scale.

The hardness of minerals has been discussed in an excellent paper by Talmage.[2]

Due principally to the different degrees of plastic flowage exhibited by extremely soft minerals, the precise comparison of their hardness is a difficult problem.

An attempt was made to obtain a quantitative relationship between the hardness of talc and indium. Sclerometer measurements using a Spencer microcharacter quickly demonstrated the futility of securing precision values for hardness when comparing a soft malleable substance with a soft partly brittle foliated one.

The microcharacter produced a clean V-shaped groove in the malleable indium but made an exceedingly irregular one as it crossed the distorted torn and upturned folia of the talc.

The scratch hardness of pure lead is only slightly lower than that of selenite. When compared with the microcharacter, the hardness of lead and selenite are so close that errors of determination may cause the values to merge with each other. The hardness of indium is so much lower than that of talc that even the sclerometer tests easily show which is harder.

Since it is possible to duplicate the hardness determinations on malleable metals with the microcharacter with satisfactory fidelity, these measurements were made on high purity lead and indium. The difference between the hardness of lead and indium is somewhat greater than the difference between the hardness of selenite and talc.

The high purity indium used in these experiments[3] contained about 0.001% lead and 0.0008% iron. Copper, silver and aluminum were present in amounts less than 0.0001%. The spectrograph showed no traces of cadmium, arsenic, thallium, tin or any other element. The hardness

[2] Talmage, S. B., Quantitative standards for hardness of the ore minerals: *Econ. Geology*, **20**, 531–553 (1925).

[3] Prepared at this laboratory by C. Zischkau.

value obtained from this indium can be regarded as identical with that of pure indium.

The lead used in the hardness comparison with indium was prepared by the writer. It contained approximately 0.00001% bismuth and 0.00005% copper. No other impurities were detected with the spectrograph.

Brinell hardness values on these metals were as follows:

	Brinell Hardness Number
High purity lead	4.0
High purity indium	0.75 (Approximate)

The microcharacter (using a 3 gram weight) produced a clean V-shaped mark as it traversed the metal specimens. On the mineral specimens it made a jagged, irregular mark bounded by torn and bent and up-turned folia. The widths of the grooves were as follows:

	mm.
Indium	0.089
Talc	0.083–0.086
Lead	0.037
Selenite	0.035–0.037

The microcharacter tests were made on metal surfaces prepared with the microtome. The widths of the grooves were measured by projecting their images on the photographic screen of the large metallographic microscope and comparing with that of the projected micrometer scale.

Microcharacter readings on high purity lead varied somewhat depending on the nature of the surface tested. Exterior chilled surfaces gave readings as low as 0.029 mm. However, surfaces of lead from the interior of a casting, prepared with the microtome, gave consistent groove widths of 0.037 mm.

Microcharacter tests on indium were consistent regardless of the flat surface selected for study. Specimens of metallic indium containing about 0.01–0.02% each of cadmium, lead, thallium, and tin gave the same hardness values as the purified specimen.

NOTES AND NEWS

CELESTITE FROM LIVINGSTON COUNTY, KENTUCKY*

G. C. Hardin, Jr., and W. R. Thurston,
U. S. Geological Survey, Washington, D. C.

Celestite which has not been hitherto reported from the Kentucky-Illinois fluorspar district, was found during the past year at the Jameson prospect, 8 miles northwest of Salem, Livingston County, Kentucky. It occurs as a small stringer in calcite.

The celestite stringer was encountered at a depth of 30 feet in the shaft. The miners, believing that the material was fluorite, brought a specimen to the writers who determined the mineral to be celestite. Possibly this mineral has been overlooked in this district in the past because of its physical resemblance to fluorite.

The celestite-bearing vein occurs in fault No. 20[1] which is in the Golconda quadrangle, Livingston County, Kentucky. The fault strikes N. 10° W. at the Jameson prospect, and the nearly vertical fault plane dips slightly westward. The fault brings into contact at the surface the Bethel sandstone and the Renault formation, of Mississippian age. The stratigraphic displacement is about 60 feet. The vein is about $4\frac{1}{2}$ feet wide and consists mainly of limestone-calcite breccia and some gouge. Along the footwall is a persistent calcite veinlet 18 to 20 inches wide. The celestite stringer was pockety, averaging 1 to 2 inches in thickness. It cut through the shaft and passed into the rock on each side so the linear extent could not be measured. The veinlet did not persist in depth, having a vertical extent of only 10 feet. That part of the stringer seen consisted chiefly of small celestite crystals and crystal aggregates lining a narrow fissure in the limestone-calcite breccia. Fluorite did not occur in the vein until a depth of 60 feet was reached, but several vugs filled with small quartz crystals were noted. Below 60 feet, the vein is 2 to 4 feet wide and is composed largely of massive brown fluorite with fine-grained barite and disseminated marcasite. A drift on the 100-foot level has been driven northwest for about 120 feet in this material but no more celestite was found.

The light sky-blue celestite is chiefly in distorted tabular crystals, about 2 centimeters wide and half a centimeter thick, and in crystalline aggregates. When the crushed mineral was examined in oils, it exhibited

* Published by permission of the Director, Geological Survey, United States Department of the Interior, Washington, D. C.

[1] Weller, Stuart, Geology of the Golconda Quadrangle: *Ky. Geol. Survey*, p. 125 (1921).

the typical (001) and (110) cleavages and a moderate transparency. Optical characteristics observed on the specimens from Kentucky are given below and are essentially identical with those published for normal celestite:

$$\alpha = 1.622, \quad \beta = 1.624, \quad \gamma = 1.630, \quad 2V = 51°,$$

optically positive, distinct dispersion $r < v$.

The celestite is believed to have been deposited by hydrothermal solutions closely allied to those depositing the fluorspar ore bodies of the district.

DIHYDRITE FROM MINERAL COUNTY, NEVADA

Hatfield Goudey, *Yerington, Nevada.*

Emerald green to blackish green, minutely botryoidal crusts in the outcrop of the Calavada Mine, Mineral County, Nevada, appeared somewhat different from the malachite and chrysocolla common to the area. The first supposition was that the mineral might be conichalcite.

Mean refractive index determined by immersion is about 1.76. Microchemical tests using potassium mercuric thiocyante, ammonium molybdate, magnesium sulfate and silver nitrate showed copper and phosphate with a little arsenate. Traces of calcium and iron, probably due to admixed impurities, were also found.

Under the binocular microscope the mineral appears as very shiny, transparent botryoidal forms with no apparent crystalline structure. With high magnification under the polarizing microscope a radiating subfibrous structure and strong anisotropism are observed.

The above characteristics agree with those published for dihydrite and no other known mineral. It may be of interest that specimens from this locality, as observed under the binocular, are very similar to those from New Jersey.

OCCURRENCE OF NEMALITE IN ALASKA*

William C. Fackler,
University of Alaska, College, Alaska.

The first Alaskan occurrence of nemalite, the fibrous variety of brucite, was found by Mr. Eskil Anderson, Associate Mining Engineer, Department of Mines, Territory of Alaska, while examining tremolite and chrysotile asbestos deposits in the Kobuk River valley. Upon the con-

* Published by permission of Mr. B. D. Stewart, Commissioner, Department of Mines, Territory of Alaska.

clusion of the 1944 field season, samples of the mineral were brought to the School of Mines, University of Alaska, for examination. In addition, samples were sent to Drs. F. F. Grout and J. W. Gruner of the University of Minnesota and to Mr. C. S. Ross and Miss Jewell Glass of the U. S. Geological Survey for examination and further investigation.

Mr. Anderson[1] found "the nemalite to be common in the asbestos deposits on Shungnak River and Cosmos Creek, about ten miles above their mouths. In both places it has been found in serpentine where it is closely associated with chrysotile. The only fibrous brucite that I observed in place was in pockets in sheared serpentine. The pockets were usually from one to three inches thick and up to a foot or two long as exposed. When the asbestos zone is more thoroughly examined, nemalite could probably be found in many places between Jade Mountain and the Kogoluktuk River."

Megascopically the specimen is composed of aggregates of hair-like fibers, eight to nine inches long, with such perfect cleavage that very fine filaments may be separated from the specimen. It is colorless to grayish or greenish white. Luster is vitreous to pearly. Fibers are brittle and transparent.

It is completely soluble in cold hydrochloric acid. Infusible, giving a brilliant incandescence. Contains a large amount of water and some iron. The presence of iron is at least partly accounted for by small inclusions of magnetite.

The mineral is optically[2] biaxial positive with 2V varying from 30° to 70°, but commonly about 30°. Good interference figures well centered were frequently observed. Parallel extinction with X parallel to the elongation of the fibers. Indices of refraction[3] are: $\alpha = 1.565$, $\beta = 1.571$, $\gamma = 1.584$; $B = .019$. The birefringence and anomalous interference colors are those of ordinary brucite.

Dr. J. W. Gruner[4] of the University of Minnesota reports that "the x-ray pattern of this mineral checks line for line with brucite."

[1] Personal communication.

[2] Optical determinations by Mr. C. S. Ross and Miss Jewell Glass of the U.S.G.S., Dr. F. F. Grout of the University of Minnesota, and the author.

[3] Determined by Mr. C. S. Ross and Miss Jewell Glass.

[4] Personal communication.

NOMINATIONS FOR OFFICERS OF THE MINERALOGICAL SOCIETY OF AMERICA FOR 1946

The Council has nominated the following for officers of The Mineralogical Society of America for the year 1946:

PRESIDENT: Paul F. Kerr, Columbia University, New York City.

VICE-PRESIDENT: S. B. Hendricks, Bureau of Plant Industry, U. S. Department of Agriculture, Beltsville, Maryland.

SECRETARY: C. S. Hurlbut, Jr., Harvard University, Cambridge, Mass.

TREASURER: Earl Ingerson, Geophysical Laboratory, Washington, D. C.

EDITOR: Walter F. Hunt, University of Michigan, Ann Arbor, Michigan.

COUNCILOR (1946–1949): Joseph Murdoch, University of California at Los Angeles, Los Angeles, California.

PROPOSED CHANGE IN THE BY-LAWS OF THE MINERALOGICAL SOCIETY OF AMERICA

The Council of the Mineralogical Society of America has approved the following change in Article IV, Section 2 of the By-Laws of the Society:

From

The list of nominations for fellowship in the Society shall be sent to the fellows at the same time as the nominations for officers. Five opposing votes shall be considered as rendering a candidate ineligible for fellowship.

To

The list of nominations for fellowship in the Society shall be sent to the fellows at the same time as the nominations for officers. If ten per cent of the fellows voting on a given candidate cast opposing votes, the candidate shall be considered ineligible for fellowship.

Members and fellows will be asked to vote on this proposed change at the time of the annual election of officers.

C. S. HURLBUT, JR., *Secretary.*

ANNOUNCEMENT OF ANNUAL MEETING

The annual meeting of the society will be held in Pittsburgh, Pennsylvania, December 27–29, 1945, in connection with the meeting of the Geological Society of America.

Members of the society who are planning to present papers at the scientific sessions of the annual meeting should notify the secretary as soon as possible in order to receive proper blanks for their abstracts. All abstracts should be in the secretary's office by *November 5, 1945.*

Advance announcement of the annual meeting was distributed to

members of the society, together with the ballot for officers, the middle of October. The final program of the meeting, including the schedule of papers, abstracts, and other information will be sent to each member in December. Further specific information regarding the annual meeting may be obtained from the secretary's office.

C. S. HURLBUT, JR., *Secretary*

NEW MINERAL NAMES

Hedleyite

H. V. Warren and M. A. Peacock: Hedleyite, a new bismuth telluride from British Columbia, with notes on wehrlite and some bismuth-tellurium alloys. *Univ. Toronto Studies*, Geol. Ser. No. **49**, 55–69 (1945).

Crystallography: Rhombohedral.

Structure cell = a_{rh} 39.68Å, $\alpha = 6°26\frac{1}{2}'$ (corresponding to the hexagonal cell a 4.46Å., c 118.8Å.); the rhombohedral unit cell contains 20 atoms or approximately $Bi_{14}Te_6$. This superlattice accounts for all lines in the x-ray pattern; a simpler cell a_{rh} 3.248Å., $\alpha = 86°42\frac{1}{2}'$, containing 1 (Bi,Te) accounts for all but two lines.

Habit: As plates up to 6 mm. wide and 1 mm. thick.

Physical Properties: Cleavage basal, easy, giving flexible and slightly elastic folia. Hardness = 2. G. = 8.68–8.93 (8.93 calcd. from x-ray data). Luster metallic, color tin white with iron-black tarnish. Opaque. By reflected light white in color and weakly anisotropic. Etch tests are given.

Chemical Properties: Analyses by G. S. Eldridge of two samples gave Bi 80.60, 81.55; Te 18.52, 17.60; S 0.12, 0.04; sum 99.24, 99.19. Spectrographic analysis of the first sample gave Sb 0.05, Pb 0.01, Cu 0.01 per cent. This is nearest to Bi_5Te_2, but Bi_7Te_3 is in better agreement with the requirements of the unit cell. Study of the system Bi-Te shows that hedleyite is a solid solution of Bi in Bi_2Te_3. The Bi content is in excess of the maximum content under stability conditions.

Occurrence: From the Good Hope mineral claim, about four miles southeast of Hedley, Osoyoos mining district, British Columbia. The country rock is a skarn composed mainly of garnet, epidote, and pyroxene, cut by irregular veins and stringers of quartz. Most of the hedleyite samples were in these quartz bodies, but some also was noted in the skarn. Associated minerals include bismuth, joseite, pyrrhotite, arsenopyrite, calcite, and gold.

Name: For the locality.

Michael Fleischer

Correction

Volume 29, page 444, Fig. 1, N_F should be interchanged with N_C, and F with C.